Geophysical Journal International

Geophys. J. Int. (2010) **182,** 631–651 doi: 10.1111/j.1365-246X.2010.04663.x

Morphology and tectonics of the Andaman Forearc, northeastern Indian Ocean

James R. Cochran

Lamont-Doherty Earth Observatory of Columbia University, 61 *Route* 9W, *Palisades,* NY 10964, *USA. E-mail: jrc@ldeo.columbia.edu*

Accepted 2010 May 17. Received 2010 April 12; in original form 2009 June 29

SUMMARY

The Andaman Sea has developed as the result of highly oblique subduction at the western Sunda Trench, leading to partitioning of convergence into trench-perpendicular and trench-parallel components and the formation of a northward-moving sliver plate to accommodate the trench parallel motion. The Andaman forearc contains structures resulting from both components of motion. The main elements of the forearc are the accretionary prism and outerarc ridge, a series of forearc basins and major N–S faults. The accretionary prism is an imbricate stack of fault slices and folds consisting of ophiolites and sediments scrapped off the subducting Indian Plate. The western, outer slope of the accretionary prism is very steep, rising to depths of 1500–2000 m within a distance of 30 km. There is a difference in the short wavelength morphology between the western and eastern portions of the accretionary prism. The outer portion consists of a series of faulted anticlines and synclines with amplitudes of a few 100 to ∼1000 m and widths of 5–15 km resulting from ongoing deformation of the sediments. The inner portion is smoother with lower slopes and forms a strong backstop. The width of the deforming portion of the accretionary prism narrows from 80 to 100 km in the south to about 40 km between 10°N and 11° 30′N. It remains at about 40 km to ∼14°40′N. North of there, the inner trench wall becomes a single steep slope up to the Myanmar shelf. The eastern edge of the outerarc ridge is fault bounded and, north of the Nicobar Islands, a forearc basin is located immediately to the east. A deep gravity low with very steep gradients lies directly over the forearc basin. The West Andaman Fault (WAF) and/or the Seulimeum strand of the Sumatra Fault System form the boundary between the Burma and Sunda plates south of the Andaman spreading centre. The WAF is the most prominent morphologic feature of the Andaman Sea and divides the sea into a shallow forearc and a deeper backarc region. The Diligent Fault runs through the forearc basin east of Little Andaman Island. Although it has the general appearance of a normal fault, multichannel seismic data show that it is a compressional feature that probably resulted from deformation of the hanging wall of the Eastern Margin Fault. This could occur if the forearc basins were formed by subduction erosion of the underlying crust rather than by east–west extension.

Keywords: Seismicity and tectonics; Subduction zone processes; Continental tectonics: strike-slip and transform; Indian Ocean.

1 INTRODUCTION

The Western Sunda Trench/Andaman Sea system is the 'type example' of strain partitioning as the result of oblique convergence, leading to trench-parallel shear in the overriding plate (Fitch 1972). Convergence between the Australian/Indian and Eurasian/Southeast Asian/Sunda plates is nearly orthogonal to the trench south of Java, but becomes progressively more oblique to the west and is nearly transcurrent west of the northern Andamans and Myanmar (e.g. Curray *et al.* 1979; McCaffrey 1991, 1996; Socquet *et al.* 2006) (Fig. 1). Shear in the overriding plate is accommodated on a variety of structures and in varying manners along the convergence zone. Jarrard (1986) referred to this type of terrain as a 'sliver plate' although they are not necessarily plates in the normal sense of being a coherent, rigid block of lithosphere. The northward moving terrain between the Indian and Sunda plates, extending from Myanmar through the western Andaman Sea and southward through the Sumatran forearc region was named the Burma Plate by Curray *et al.* (1979).

The trench-parallel component of motion in Sumatra is largely accommodated by strike-slip motion on the Sumatran fault (Curray *et al.* 1979; McCaffrey 1991; Genrich *et al.* 2000; Sieh & Natawidjaja 2000) located near the volcanic arc. An additional, smaller component occurs offshore, along faults such as the

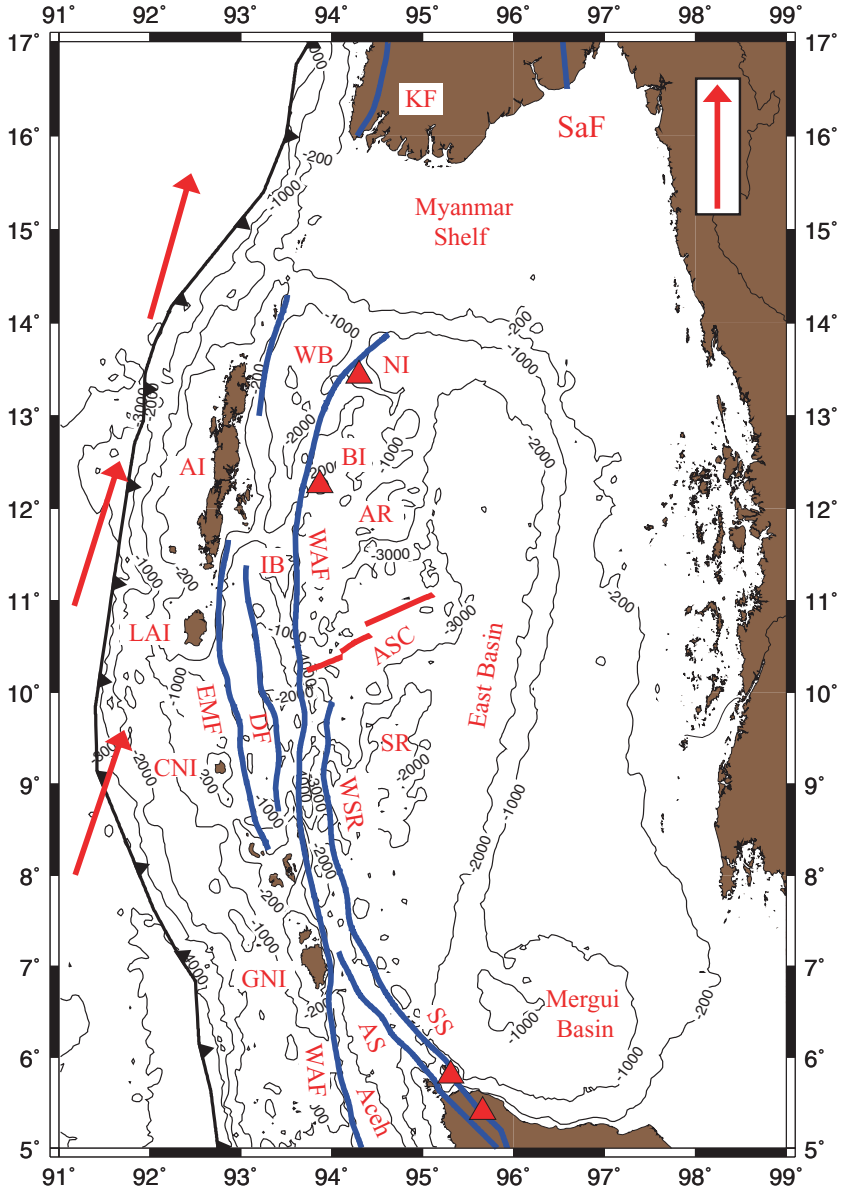

Figure 1. Map showing the location of geographic features mentioned in the text. Red arrows show the convergence direction and rate between the Indian Plate to the west and the Sunda Plate to the east of the Burma Plate using the pole of Socquet *et al.* (2006). Scale is given by the arrow in the inset which has an amplitude of 30 mm a^{-1}. Red triangles show the location of subaerial volcanoes. Aceh, Aceh Forearc Basin; AI, main Andaman Island group (Lower Andaman, Middle Andaman and North Andaman Islands); AR, Alcock Rise; AS, the Aceh strand of the Sumatran Fault System; ASC, the Andaman spreading centre; BI,Barren Island; CNI, Car Nicobar Island; DF, the Diligent Fault; EMF, the Eastern Margin Fault; GNI, Great Nicobar Island; IB, Invisible Bank; KF, the Kabaw Fault; LAI, Little Andaman Island; NI, Narcondam Island; SaF, the Sagaing Fault; SR, Sewell Rise; SS, the Seulimeum strand of the Sumatran Fault System; WAF, the West Andaman Fault; WB, West Basin; WSR, the West Sewell Ridge.

Mentawai fault (Diament *et al.* 1992) and/or as distributed shear strain in the fore arc region (Genrich *et al.* 2000; McCaffrey *et al.* 2000). The principal boundary between the Sunda and Burma plates in the southern Andaman Sea is formed by the Seulimeum strand of the Sumatran Fault and/or the West Andaman Fault (WAF), which intersects the Aceh strand of the Sumatran Fault near 7°N to the east of Great Nicobar Island (Fig. 1). The WAF intersects the southwest end of the Andaman spreading centre near 10°15′N (Curray *et al.* 1979). The spreading centre, presently spreading at 38 mm a^{-1} (Kamesh Raju *et al.* 2004), extends for ∼175 km nearly perpendicular to the trench. From its northeast end, a system of transforms and short spreading centres extends the plate boundary to the Sagaing fault, which forms the boundary between the stable Sunda Plate and the deforming region in Myanmar (e.g. Curray *et al.* 1979; Guzman-Speziale & Ni 1993; Curray 2005; Socquet *et al.* 2006). Recent motion across the Sagaing fault is measured at about 18 mm a^{-1} (Vigny *et al.* 2003) or about half of the total motion.

The forearc region, to the west of the WAF and the Sumatran fault system, immediately overlies the rupture zone of the great 2004 December 26 earthquake (Ammon *et al.* 2005; Lay *et al.* 2005). Shallow earthquakes prior to the 2004 December earthquake delineate the plate boundary and are concentrated along the WAF and/or Seulimeum fault to the south of 10°N and the spreading centre and its continuation through the backarc towards the Sagaing fault in Myanmar to the north of 10°N, with scattered pockets of epicentres farther west (Fig. 2a). In contrast, aftershocks of the 2004

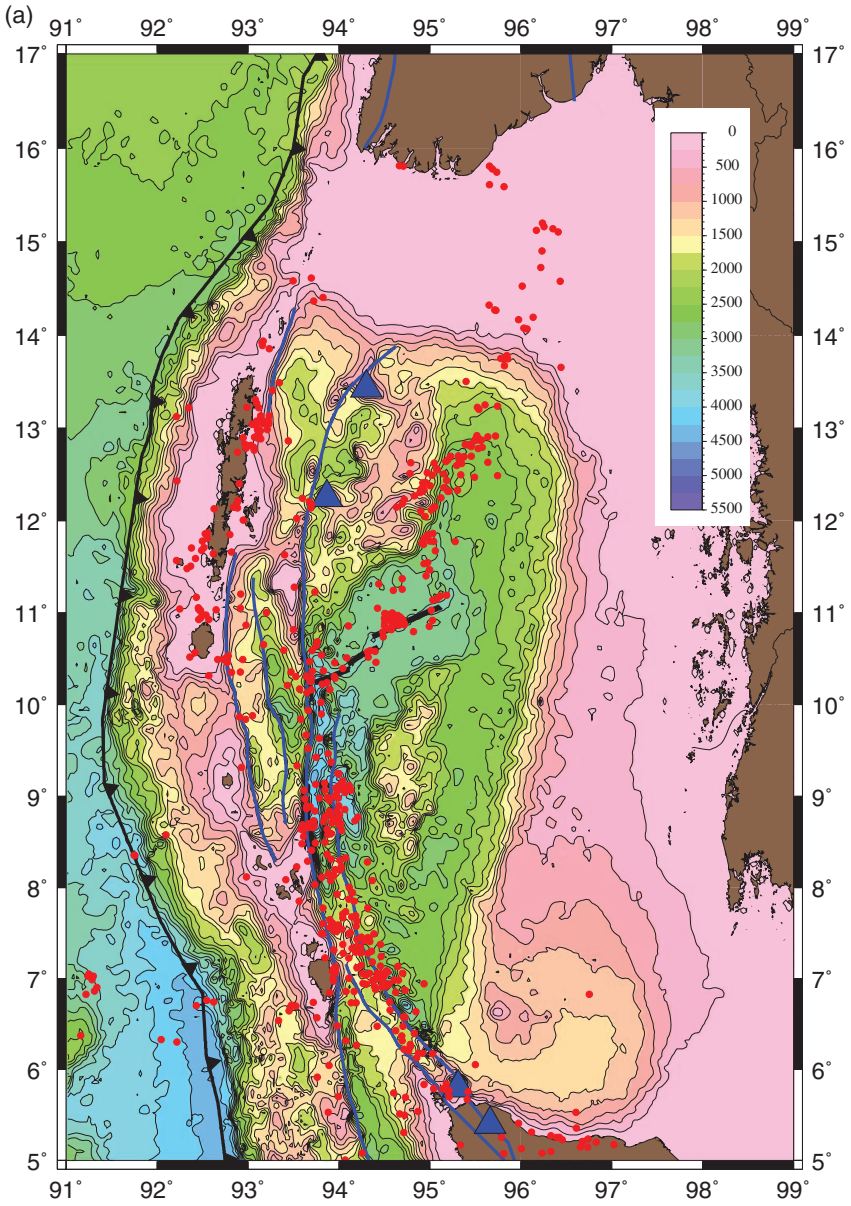

Figure 2. Location of earthquakes in the Andaman Sea occurring at depths shallower than 35 km: (a) from 1918 to 2005 December 25 relocated using the EHB technique by Engdahl *et al.* (2007) and (b) between the great earthquakes of 2004 December 26 and 2005 March 27 relocated using the EHB technique by Engdahl *et al.* (2007). Major faults are shown in blue. Blue triangles show locations of subaerial volcanoes. Bathymetry is derived from satellite altimetry (Smith & Sandwell 1997) and is contoured at 250 m intervals. Insert gives bathymetry colour scale in metres.

December 26 earthquake are almost entirely located on and to the west of the Seulimeum fault and are widely distributed through the forearc (Fig. 2b), reflecting interactions with the subducting slab. Since 2006, the distribution of shallow earthquakes has basically returned to the pre-2004 pattern.

The tectonic regime in the Andaman Sea has varied in time as the geometry of the convergence zone has evolved. Curray (2005) outlined a multiphase history involving several episodes of back arc extension since the middle Eocene in response to the evolving geometry as the subduction zone rotated clockwise in response to the northward penetration of India. Curray's (2005) synthesis provides an extremely valuable framework for understanding the geological history and development of the Andaman Sea. However, since Curray's (2005) primary focus was on understanding the history and development of the Andaman Sea, he concentrated on elements of the geology and the geophysics of the backarc region that are critical to that objective. The purpose of this paper is to assemble all available geophysical data to systematically define the morphology, structure and tectonics of the Andaman forearc region.

2 AVAILABLE DATA

Ship tracks for marine geophysical data available for this study are shown in Fig. 3. This includes all data accessible through the National Geophysical Data Centre (NGDC) and additional lines available at LDEO. A major source of data is a series of Scripps cruises from 1963 to 1979 (Curray *et al.* 1979; Curray 2005). Other significant data sources are cruises carried out by LDEO, the US Navy and NOAA. Bathymetry data north of 7°N are all single-beam

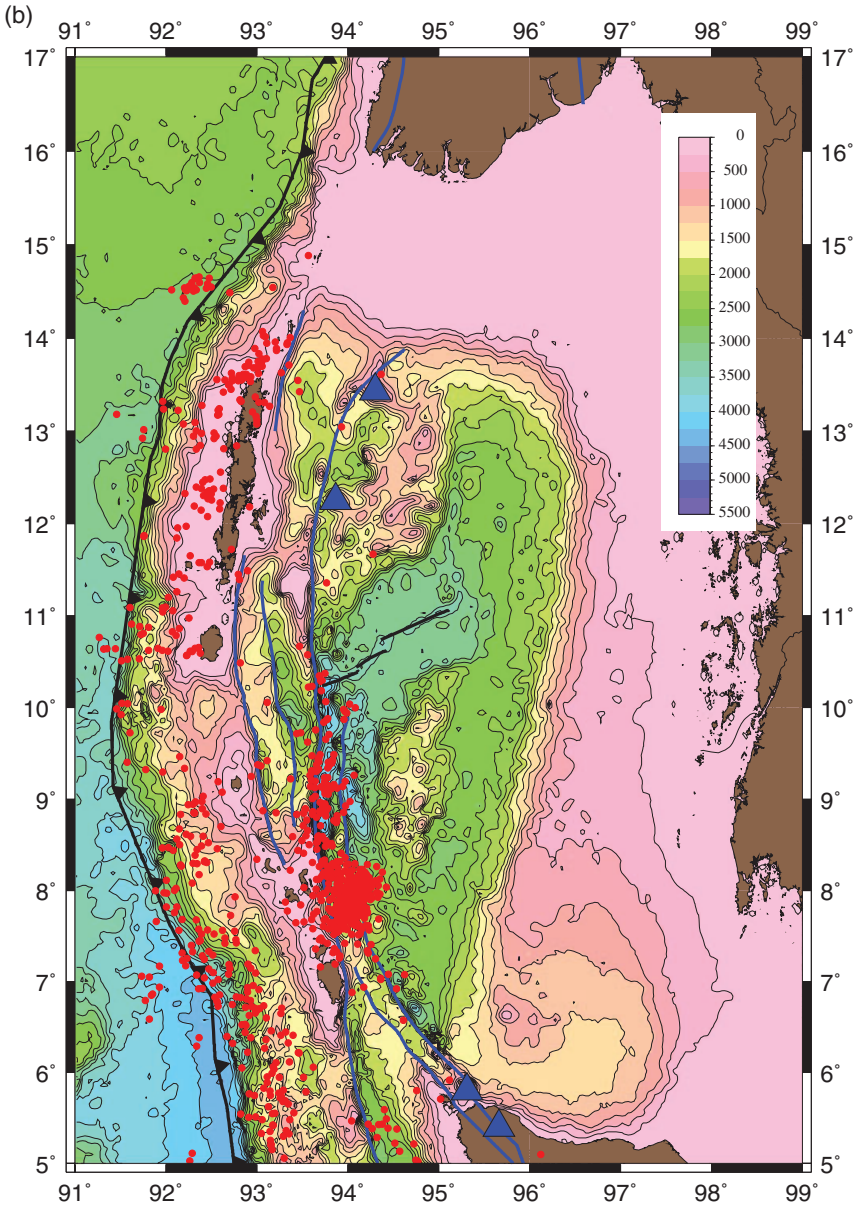

Figure 2. (*Continued.*)

echo sounder data, reflecting the fact that non-Indian investigators have not been able to collect data in the Andaman Sea for many years, so most of the available data in Indian waters is pre-1985. Gravity and magnetics data are also available for many of these lines. Seismic reflection data, primarily analogue single-channel data, are available from some of the cruises.

Gridded multibeam data collected during cruises to the forearc area to the west and northwest of the location of the great 2004 December 26 earthquake (e.g. Henstock *et al.* 2006; Sibuet *et al.* 2007; Graindorge *et al.* 2008) are also available. In particular, *R/V Marion Dufresne* surveyed an ∼80-km-wide band extending for >300 km from NE of the Sumatran Fault System between Sumatra and Nicobar across the forearc region to undisturbed seafloor seaward of the trench (Sibuet 2005). The area covered by this survey is shown in light blue in Fig. 3 and extends to the SW off of the figure.

I also have a grid of oil industry multichannel seismic reflection lines in the forearc basin immediately east of Little Andaman Island (Figs 1 and 4) that served as the site survey for Site NGHP-1-17 (Collett *et al.* 2008a,b).

3 GEOLOGICAL DEVELOPMENT OF THE ANDAMAN SEA

The Andaman Sea can be broadly divided into forearc and backarc regions by the WAF and the Sumatran fault system. The main feature of the forearc is the Andaman–Nicobar ridge, which includes the accretionary prism of the subduction zone. Throughout most of the area, a forearc basin bounds the Andaman–Nicobar Ridge on the east. The backarc region consists of features developed during different phases in the evolution of the Burma Plate.

There is no prominent volcanic arc. Barren Island, near 12°18′N, 93°49′E, and Narcondam Island, near 13°16′N, 94°18′E (Fig. 1) are the only subaerial volcanoes in the Andaman Sea. Volcanic activity,

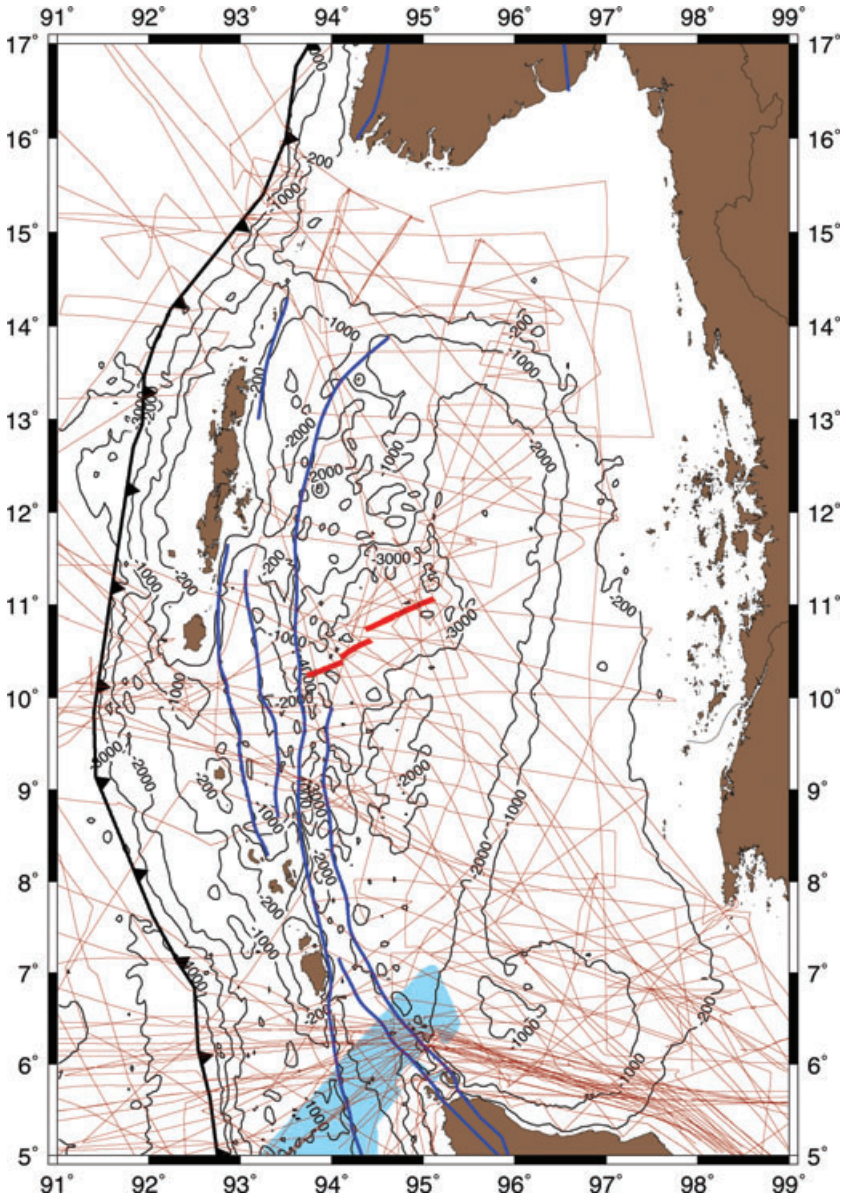

Figure 3. Track chart showing location of shipboard geophysical data utilized in this study. Light blue shading shows location of multibeam swath bathymetry data collected by *R/V Marion Dufresne* (Sibuet 2005) (Figs 11 and 14). Major faults are shown as heavy blue lines. The Andaman spreading centre is shown in heavy red lines.

perhaps precipitated by the 2004 earthquake, was observed on Barren Island in 2005 (Laluraj *et al.* 2006). Its last previous eruption was in 1994. There are no historic reports of eruptions on Narcondam. Andesite and dacite are found on Narcondam and basalt on Barren Island (Washington 1924; Pal *et al.* 2007). Both are isolated volcanic seamounts and are located just east of the WAF to the north of the Andaman spreading centre. Rodolfo (1969) and Curray (2005) both report the presence of seamounts that may be volcanoes in a similar setting further south. In spite of the apparent lack of volcanism, volcanic ash is observed either as beds or disseminated through sediments throughout a 700-m-long core recovered by *R/V JOIDES Resolution* at Site NGHP-1–17 located near 10°45′N, 93°7′E, ∼55 km east of Little Andaman island (Johnson *et al.* 2007; Collett *et al.* 2008b) as well as ashore on the Andaman Islands (Pal *et al.* 2005).

3.1 Morphology and geological development of the backarc region

Present backarc extension is centred at the Andaman spreading centre which intersects the WAF near 10°15′N, 93°40′E and extends ENE from there for ∼175 km (Figs 1 and 4). The spreading centre has been active for ∼4 Myr and Anomaly 2A is the oldest confidently identified magnetic anomaly (Kamesh Raju *et al.* 2004). Kamesh Raju *et al.* (2004) suggest a present total opening rate of 38 mm a^{-1} with a slower rate of 16 mm a^{-1} prior to 2 Ma. A diffuse region of earthquake epicentres extends northward from the northeast end of the spreading centre towards the Sagaing fault in Myanmar (Fig. 2a). Curray (2005) interpreted this as a system of transforms and short spreading centres.

Morphologically, the spreading centre is marked by a 400–600-m-deep rift within a flat, sediment filled basin at a depth of

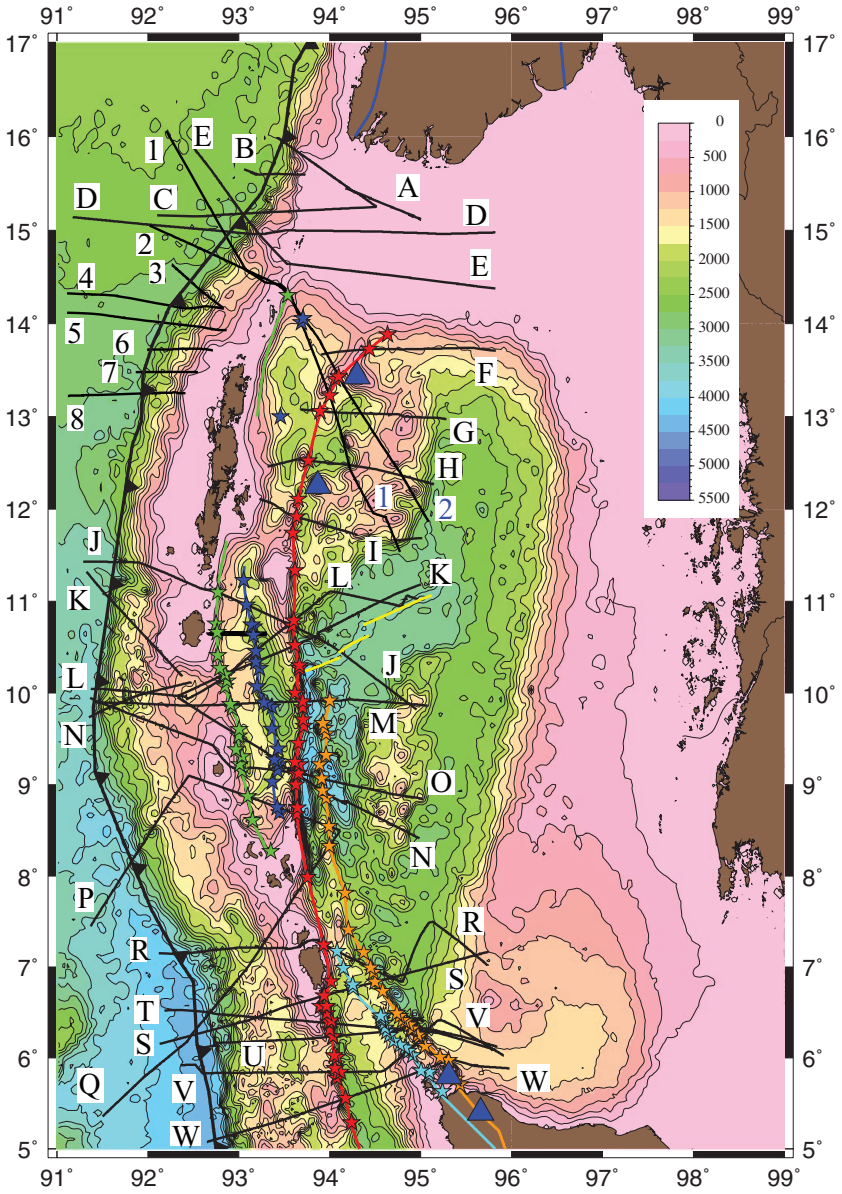

Figure 4. Bathymetry map of the Andaman Sea showing the location of major faults mapped in this study. Coloured lines show the location of the faults with stars showing the location at which they were identified on individual ship tracks. The Aceh strand of the Sumatran Fault System is shown in teal. The Seulimeum strand is shown in orange. The West Andaman Fault is shown in red. The Diligent Fault is shown in dark blue. The Eastern Margin Fault is shown in green. A northern equivalent of the EMF is also shown in green. The Andaman spreading centre (from Kamesh Raju *et al.* (2004)) is shown in yellow. Location of Kabaw and Sagaing faults in Myanmar is from Curray (2005). The figure also shows the location of ship tracks for projected profiles shown in Figs 5–8, 12 and 13. The heavy E–W line immediately east of Little Andaman Island shows the location of the seismic reflection line shown in Figs 15 and 16. Bathymetry is derived from satellite altimetry (Smith & Sandwell 1997) and is contoured at 250 m intervals. Insert gives bathymetry colour scale in metres.

~3000 m that has been flooded with sediment from the Irrawaddy River (Curray *et al.* 1979; Kamesh Raju *et al.* 2004; Curray 2005). The Andaman spreading centre runs between Alcock and Sewell Rises (Fig. 1), which comprised a single morphologic structure prior to 4 Ma. Sewell Rise extends south from the area of active seafloor spreading for about 200 km to ~8°30′N. Alcock Rise extends for a comparable distance to the north to the Myanmar margin. (Figs 1 and 4) The rises are areas of rough bathymetry at depths of 1000–2000 m that Curray (2005) described as 'not well surveyed bathymetrically'. Basalts have been recovered from Alcock Rise (Rodolfo 1969; Curray 2005) and samples from a dredge on southern Alcock Rise were dated at ~20 Ma (Curray 2005). The eastern margin of the two rises is at about 95°E (Fig. 1) and East Basin, at a depth of ~2500 m, is located between them and the Asian continental margin.

Curray (2005) proposed a geological history for the Andaman Sea involving establishment of a strike slip sliver fault in the mid-Eocene and a series of distinct episodes of backarc extension since late Oligocene in response to the trench-parallel component of stress as the trend of the western portion of the Sunda trench rotated in response to the increasing encroachment of India into Eurasia. Establishment of the current tectonic regime in the Andaman Sea began at ~4 Ma, when the present Andaman spreading centre nucleated (Kamesh Raju *et al.* 2004). An additional important development was the establishment of the Sumatran Fault System as the primary plate boundary in northern Sumatra since 2 Ma (Sieh & Natawidjaja

2000). Prior to that time, much of the offset was carried by other faults in the forearc to the west of the Sumatran Fault, including the WAF (Sieh & Natawidjaja 2000).

4 THE ANDAMAN–NICOBAR RIDGE

The principal components of the Andaman forearc are the Andaman–Nicobar Ridge, which consists of the accretionary prism and outerarc ridge, and a series of forearc basins that bound the Andaman–Nicobar Ridge on the east (Figs 1 and 4). A series of geophysical profiles across the forearc are shown in Figs 5–8 and three single-channel seismic reflection lines across it are shown in Fig. 9. The Andaman–Nicobar Ridge is an imbricate stack of fault slices consisting of slivers of seafloor ophiolites and the overlying sediments, capped by Neogene shallow water sediments (e.g. Pal *et al.* 2003). The eastern edge of the ridge is fault bounded and, north of the Nicobar Islands, forearc basins are located between the ridge and the WAF. A deep gravity low with very steep gradients lies directly over the forearc basins (Figs 4, 6, 7 and 10).

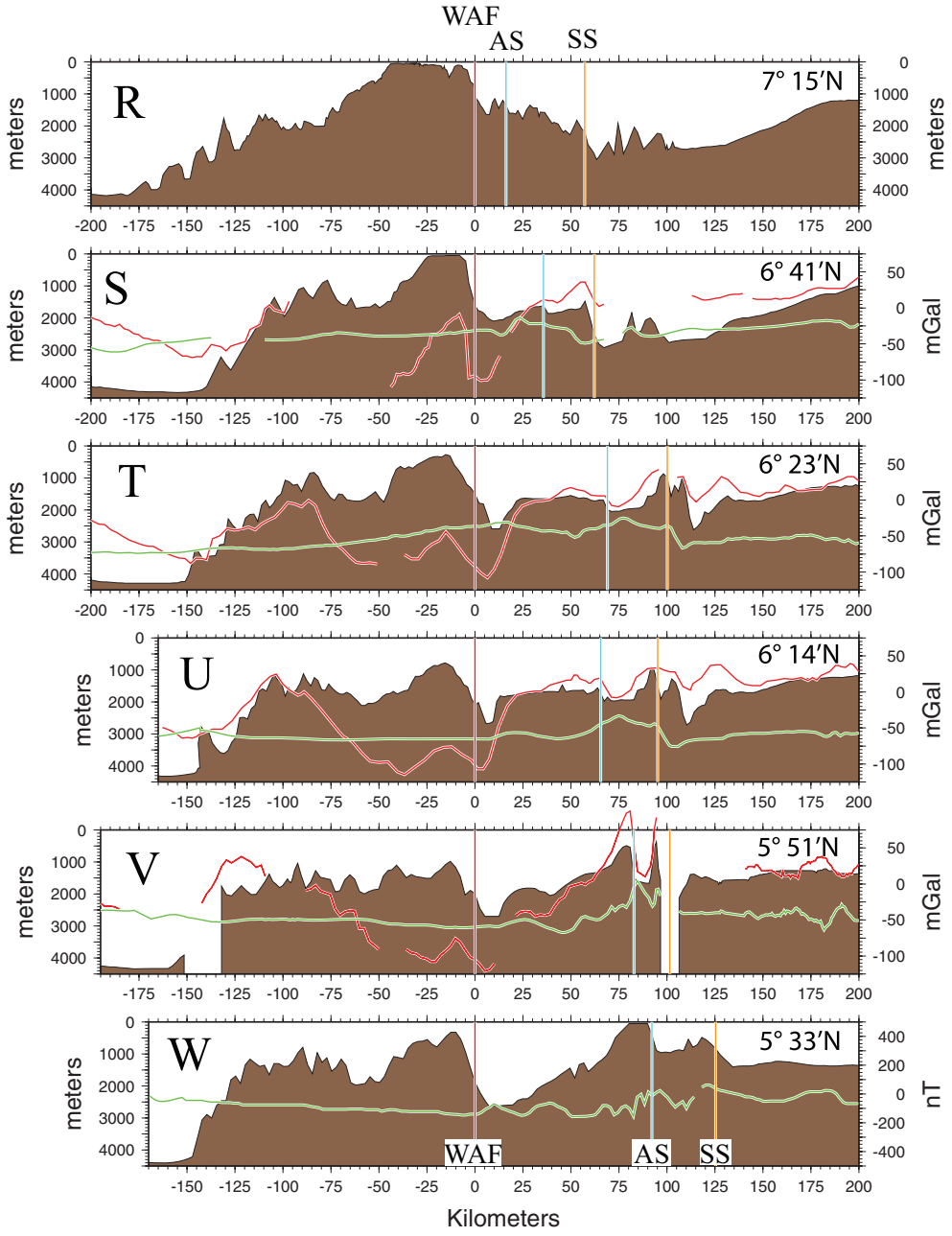

Figure 5. Shipboard geophysical profiles across the southern Andaman Sea. Letters on the profiles correspond to those on Fig. 4, which shows the ship tracks for each profile. Bathymetry is in brown, free-air gravity anomalies are in red and total intensity magnetic anomalies are in green. Profiles are projected along an east–west line with west to the left. The origin for each profile is taken as where the ship track crosses the West Andaman Ridge (WAF). Vertical lines using the same colour scheme as in Fig. 4 show the location of major north-south faults. WAF, the West Andaman Fault; AS, the Aceh strand of the Sumatran Fault System and SS, the Seulimeum strand of the Sumatran Fault System. The latitude at which each profile crosses the WAF is noted. Vertical exaggeration is 16.67:1.

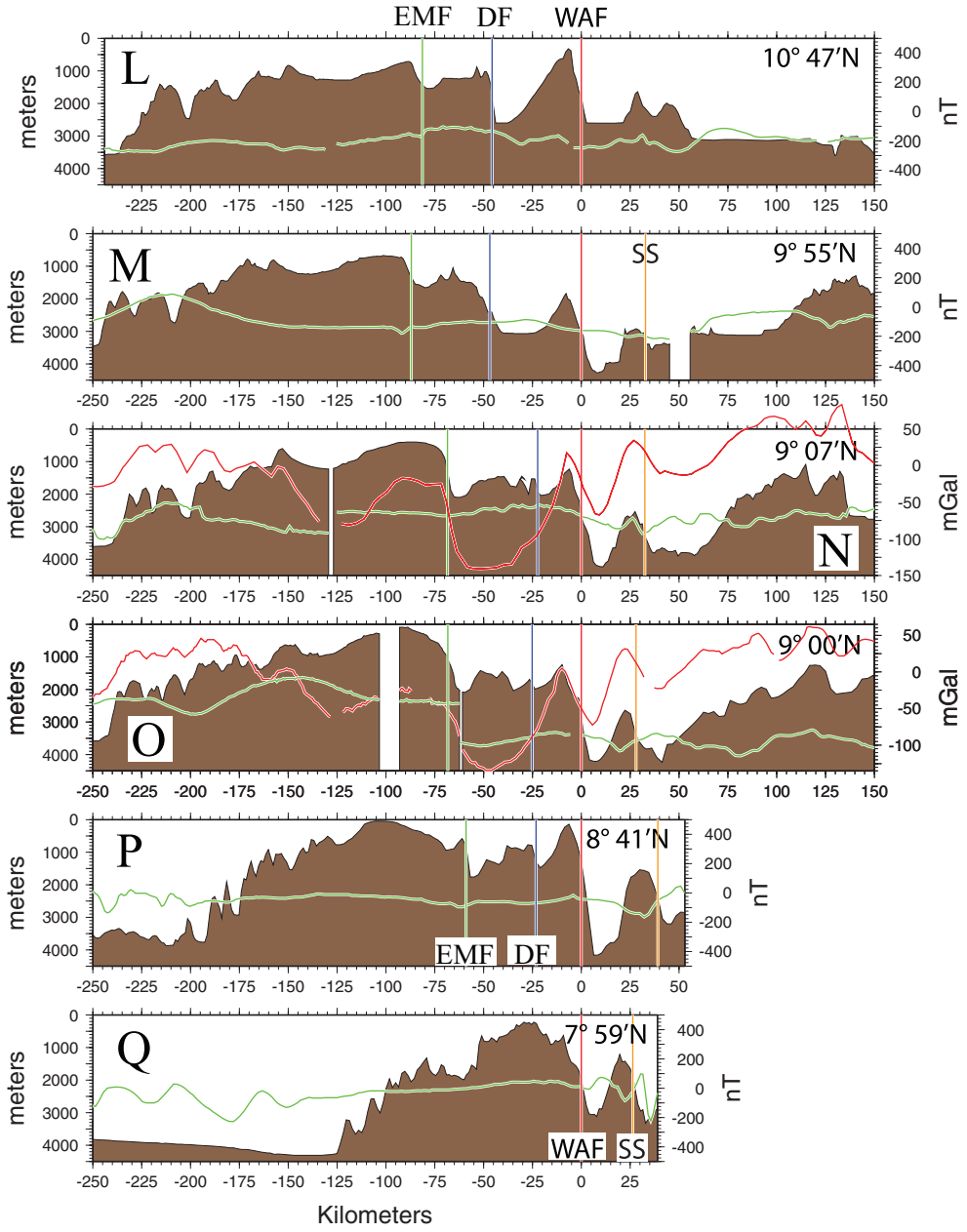

Figure 6. Shipboard geophysical profiles across the central Andaman Sea. Letters on the profiles correspond to those on Fig. 4, which shows the ship tracks for each profile. Bathymetry is in brown, free-air gravity anomalies are in red and total intensity magnetic anomalies are in green. Profiles are projected along an east–west line with west to the left. Vertical lines using the same colour scheme as in Fig. 4 show the location of major north-south faults. WAF, the West Andaman Fault; SS, the Seulimeum strand of the Sumatran Fault System; DF, the Diligent Fault and EMF, the Eastern Margin Fault. The origin for each profile is taken as where the ship track crosses the WAF. The latitude at which each profile crosses the WAF is noted. Vertical exaggeration is 16.67:1.

There are limited shipboard data available from the region of the accretionary prism and many of the ship tracks are bunched in the vicinity of shipping channels between the islands (Fig. 3). In particular, there are no shipboard data over the Andaman–Nicobar Ridge from about 11°30′N to 13° directly to the west of the Andaman Islands and only a few lines between 7°N and 9°N. However, the existing data appear sufficient to characterize the ridge and determine how its nature changes as its strike becomes more parallel to the India/Sunda relative motion (Socquet *et al.* 2006) in the north (Fig. 1).

On most profiles, the outer slope of the accretionary prism is very steep, rising from the level of the Bengal Fan sediments to a terrace at a depth of 1500–2000 m within a distance of ∼30 km (Figs 5–7). A bathymetric high, the outerarc ridge, containing the Nicobar and Andaman Islands is located along the eastern side of the prism. South of 11°N, a large gravity high is located at the seaward edge of the terrace with a smaller amplitude gravity high found over the outerarc ridge (Figs 5 and 6). The gravity high appears to broaden out north of 11°N to include the entire terrace (Fig. 10), which is very shallow in this region (Figs 4 and 7, profile J).

South of 7°N, a secondary bathymetric high is also located near the western, seaward side of the terrace, giving it a bowed or concave upward appearance (Fig. 5, profiles S–W). Similar morphology has been observed further south to the west of Sumatra in the area

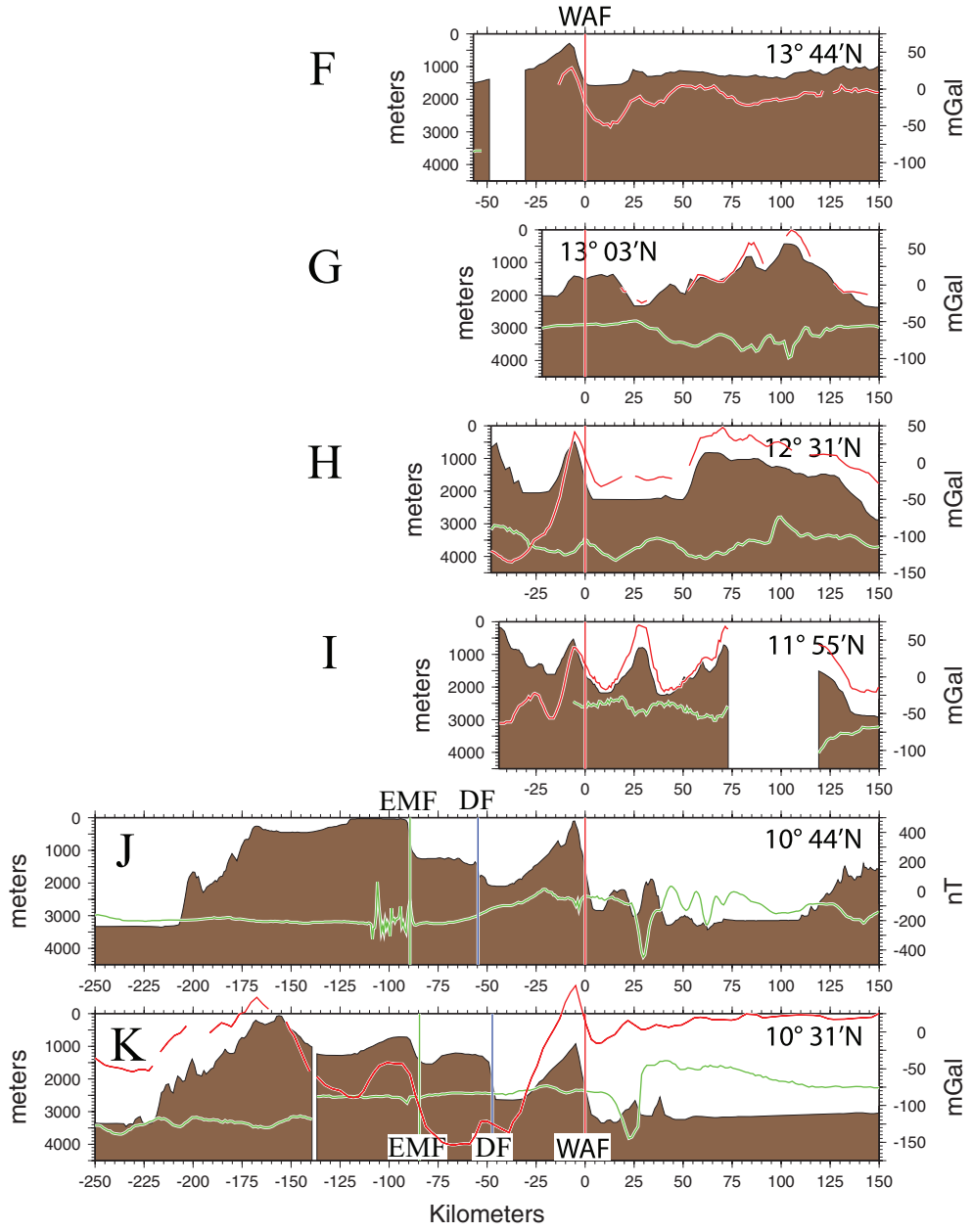

Figure 7. Shipboard geophysical profiles across the northern Andaman Sea. Letters on the profiles correspond to those on Fig. 4, which shows the ship tracks for each profile. Bathymetry is in brown, free-air gravity anomalies are in red and total intensity magnetic anomalies are in green. Profiles are projected along an east–west line with west to the left. The origin for each profile is taken as where the ship track crosses the West Andaman Ridge (WAF). Vertical lines using the same colour scheme as in Fig. 4 show the location of major north–south faults. WAF, the West Andaman Fault; DF, the Diligent Fault and EMF, the Eastern Margin Fault. The latitude at which each profile crosses the WAF is noted. Vertical exaggeration is 16.67:1.

that was extensively investigated following the 2004 December 26 earthquake (e.g. Henstock *et al.* 2006; Fisher *et al.* 2007; Sibuet *et al.* 2007; Seeber *et al.* 2007; Graindorge *et al.* 2008; Mosher *et al.* 2008; Graindorge *et al.* 2008). North of 7°N, the terrace tends to continue to shallow to the east rather than have a culmination near its seaward edge (Fig. 6, profiles L–P).

There is a distinct difference in the nature of the short wavelength morphology between the western and eastern portions of the accretionary prism. The western portion is characterized by a series of anticlines and synclines with amplitudes of a few hundred to a thousand metres and widths of 5–15 km, reflecting compressional deformation of the accreting sediments. The zone of highly deformed seafloor is 80–100 km wide to the south of 11°N. The seafloor in the eastern portion of the prism is smoother with lower slopes and bathymetric undulations are of longer wavelength (Figs 5–7 and 9). This change in the nature of the bathymetry can be clearly observed in the profiles shown in Figs 5–7 and in Fig. 11, which shows *R/V Marion Dufresne* swath bathymetry (Sibuet 2005) in a corridor from the trench to the Aceh Basin.

Sibuet *et al.* (2007) and Lin *et al.* (2009) identify the trace of a westward verging thrust fault called the ‘Upper Thrust Fault’ by Sibuet *et al.* (2007) and the ‘Upper Splay Fault’ by Lin *et al.* (2009) as located at the boundary in the form of the short wavelength bathymetry in the area of 5°N to 6°N. They both suggest that this

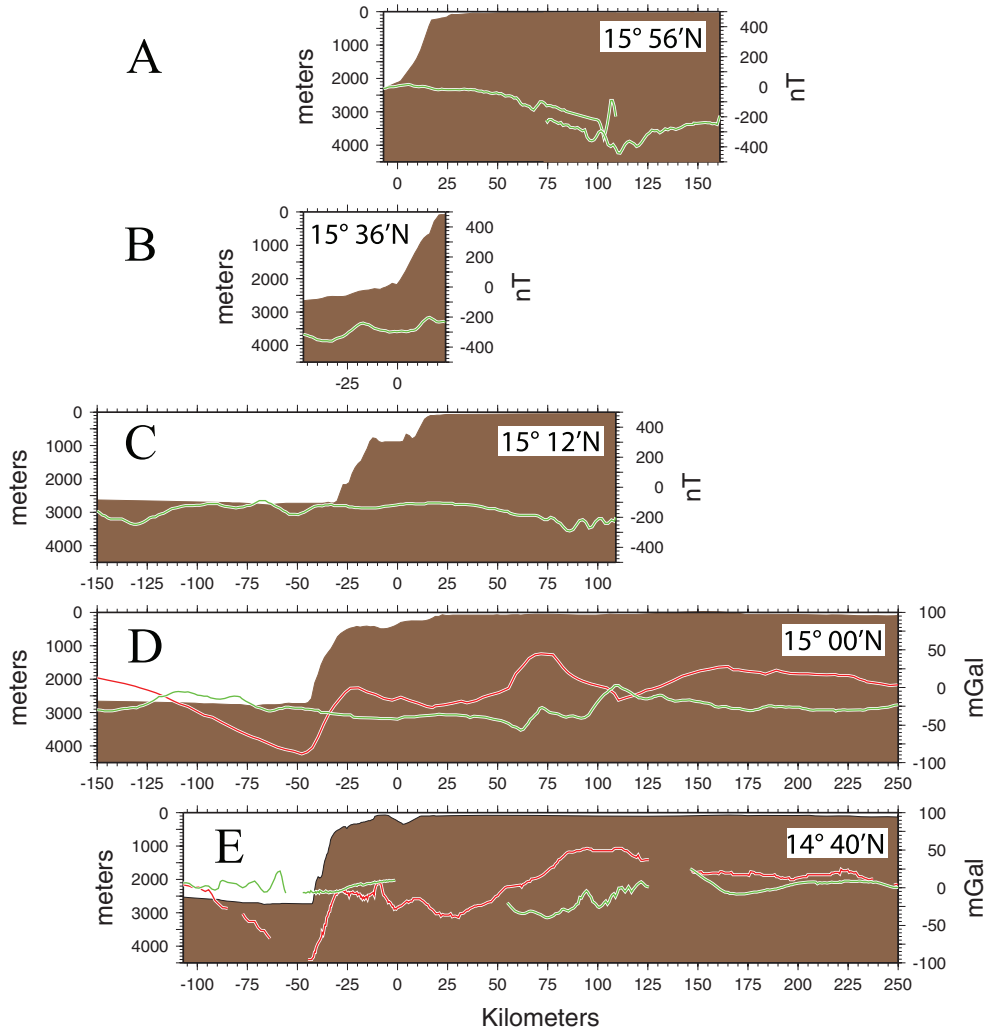

Figure 8. Shipboard geophysical profiles across the Myanmar shelf. Letters on the profiles correspond to those on Fig. 4, which shows the ship tracks for each profile. Bathymetry is in brown, free-air gravity anomalies are in red and total intensity magnetic anomalies are in green. Profiles are projected along an east–west line with west to the left. The origin for each profile is at 93°30′E and the latitude at 93°30′E is noted. Vertical exaggeration is 16.67:1.

fault may be a major splay off of the main subduction plate boundary. The fault may mark the boundary between a deforming outer portion of the accretionary prism and a stronger inner 'backstop'.

The morphology of the accretionary prism changes north of ∼11°N. The width of the outer deforming region narrows from almost 90 km on profile L (Fig. 6) at about 10°N to 70 km on profile K (Figs 7 and 9a) near 10° 45′N and to 40 km on profile J (Fig. 7) near 11°25′N. The zone of folded seafloor remains approximately 40 km wide north to about 14° 40′N (Figs 12 and 13, profile 2). North of there, the inner trench wall becomes a single steep slope up to a terrace, which shallows northward and merges into the Myanmar shelf (Fig. 13, profile 1, and Fig. 8, profiles A–E). The change in morphology of the prism between 14°N and 15°N roughly coincides in location with the northern end of the rupture zone of the 2004 December 26 earthquake (Ammon *et al.* 2005; Bilham 2005).

Profiles presented by Nielsen *et al.* (2004) show that the steep margin to the north of 15°N, which they call the West Burma Scarp, continues northward to about 18°N where the accretionary prism broadens to form the Ramree lobe of the Arakan Yoma wedge (Nielsen *et al.* 2004). From a detailed analysis of swath-bathymetry and seismic reflection data, Nielsen *et al.* (2004) argue that the relative convergence direction between the Indian Plate and the northern continuation of the Burma sliver plate west of Myanmar is ∼N35°E. Since the motion between the Indian and Sunda plates at 16°N is at N15°E (using the Socquet *et al.* (2006) pole), there is still a partitioning of the motion with a component of the India–Sunda motion occurring on N–S faults within Myanmar.

5 LARGE NORTH–SOUTH TRENDING FAULTS

A series of prominent north–south trending faults are an important component of the tectonic fabric of the forearc. The eastern boundary of the outerarc ridge is defined by large down-to-the-east faults for the entire region south of the Myanmar shelf (Fig. 4). In addition, present and past boundaries between the Sunda Plate and the northward moving Burma Plate are formed by prominent N–S trending faults. These faults generally have a clear morphologic expression (Figs 4–7). I have determined the location of the faults along the ship tracks shown in Fig. 3. The locations were determined from a combination of bathymetry, gravity and single-channel seismic reflection data. These locations are given by stars on Fig. 4 and as vertical lines on the projected profiles in Figs 5–7 and 13.

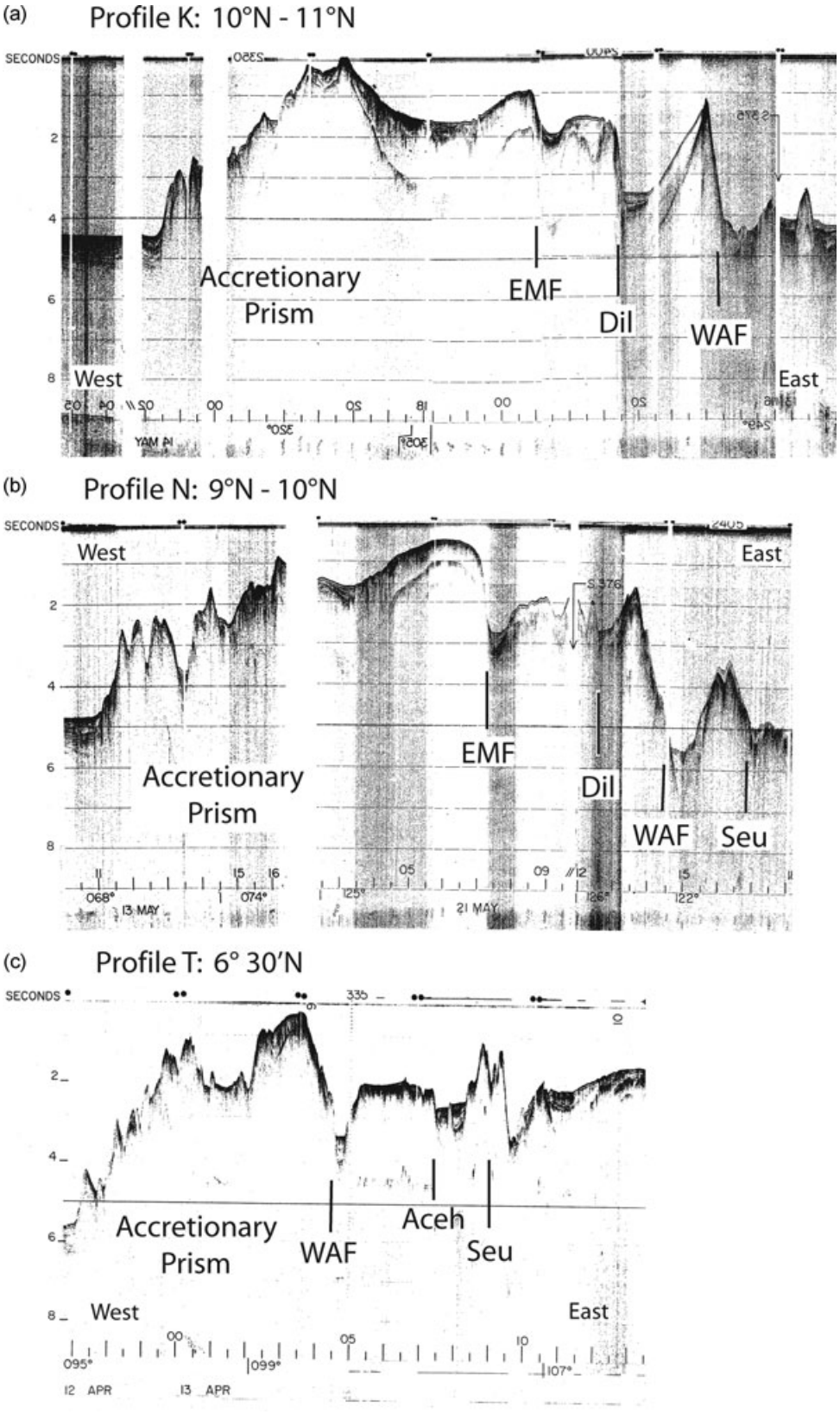

Figure 9. Single-channel seismic reflection profile across the Andaman forearc: (a) between 10°N and 11°N obtained on *R/V Robert D. Conrad* in 1973. The seismic line was collected concurrently with the geophysical data shown in profile K, Fig. 7; (b) between 9°N and 10°N obtained on R/V *Robert D. Conrad* in 1969. The seismic line was collected concurrently with the geophysical data shown in profile N, Fig. 6 and (c) near 6° 30′N obtained on *R/V Vema* in 1978. The seismic line was collected concurrently with the geophysical data shown in profile T, Fig. 5. EMF, Eastern Margin Fault; Dil, Diligent Fault; WAF, West Andaman Fault; Aceh, the Aceh strand of the Sumatran Fault System and Seu, the Seulimeum strand of the Sumatran Fault System. Vertical exaggeration is approximately 30:1.

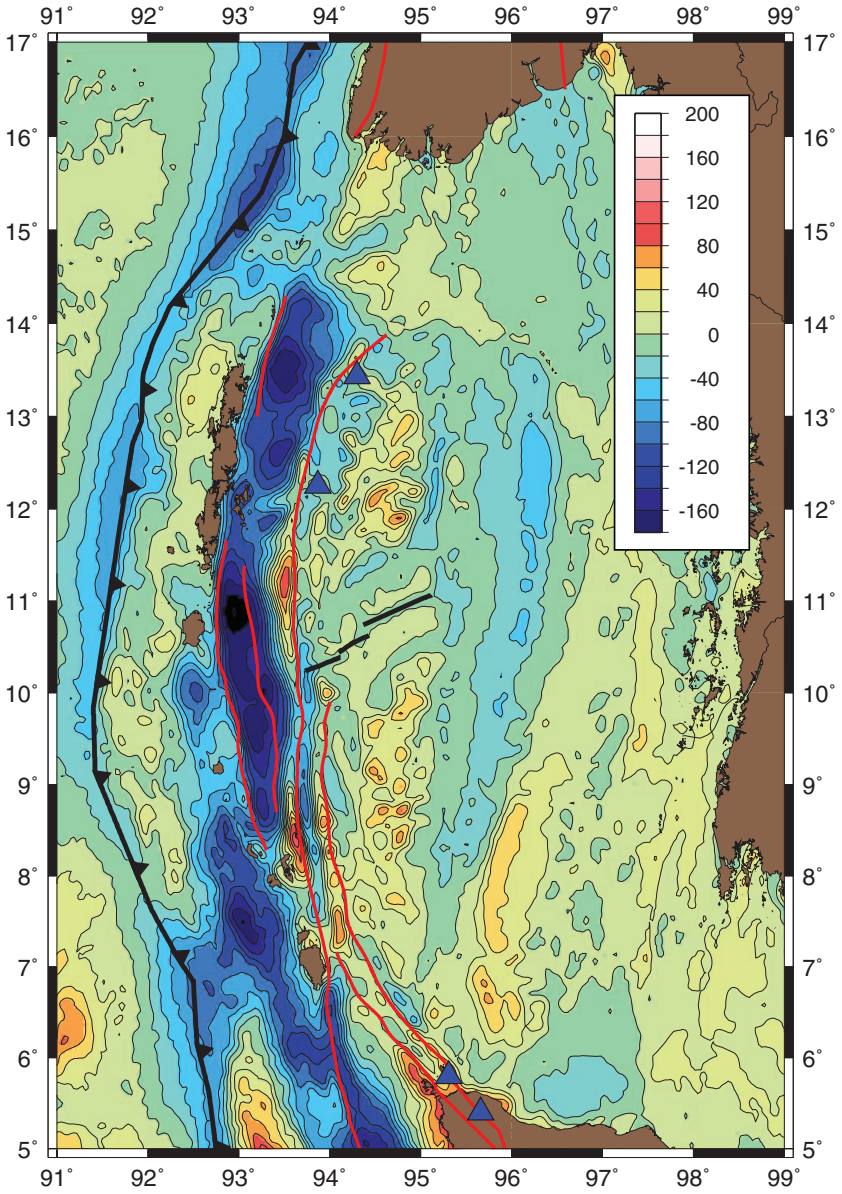

Figure 10. Free-air gravity anomaly map of the Andaman Sea contoured at 20 mGal intervals. Colour scale in mGal is given in the inset. Anomalies are determined from satellite altimetry data (Sandwell & Smith 1997, 1999). Major north-south faults are shown as heavy red lines. The Andaman spreading centre is shown as heavy black lines. Dark blue triangles show the location of subaerial volcanoes.

The Sumatran Fault forms the principal boundary between the Sunda Plate and the sliver plate in Sumatra (e.g. Curray *et al.* 1979; McCaffrey 1991; Genrich *et al.* 2000; Sieh & Natawidjaja 2000). McCaffrey *et al.* (2000) estimates that two-thirds of the total margin parallel component of plate motion in northern Sumatra is accommodated on the Sumatran Fault system with the rest occurring on offshore faults. Estimates of slip rate along the Sumatran Fault between the Equator and ∼5°N, based on both GPS and on the offset of dated features, are in the range of 22–28 mm a^{-1} (e.g. McCaffrey 1991; Bellier & Sebier 1995; Genrich *et al.* 2000; McCaffrey *et al.* 2000; Bock *et al.* 2003). North of about 5°N, the fault divides into two principal strands, the Aceh strand to the west and the Seulimeum strand to the east. Both strands can be traced north of Sumatra into the Andaman Sea. The Seulemeum strand is shown in orange and the Aceh strand in teal in Figs 4–6 and 14. North of Sumatra, both faults are expressed as steep east-facing scarps (Figs 5, 9c and 14). The scarp associated with the Aceh strand becomes less prominent north of 6°10′N. However, three LDEO seismic reflection lines that cross it between 6°10′N and 6°30′N show about 1 second two-way traveltime (twtt) of sediment in the basin between the two strands (Fig. 9c). The Aceh strand can be easily traced to about 6°50′N (Fig. 5, profile S) and with less confidence to 7°10′N. It then appears to die out or, more likely, to merge with the WAF east of Great Nicobar Island (Fig. 4).

The Seulemeum strand continues north of Sumatra as a prominent scarp, often with over 1500 m of relief, separating the forearc from East Basin (Fig. 5, profiles R–W). Near 7°30′N, this scarp merges into the east flank of a ridge, called the West Sewell Ridge by Curray (2005) (Fig. 6, profiles M–Q). The tectonic diagram of Curray (2005) shows the Seulemeum strand merging with the WAF near 9°30′N. However, shipboard geophysical profiles show that the West Sewell Ridge (and thus the Seulemeum strand that forms its eastern

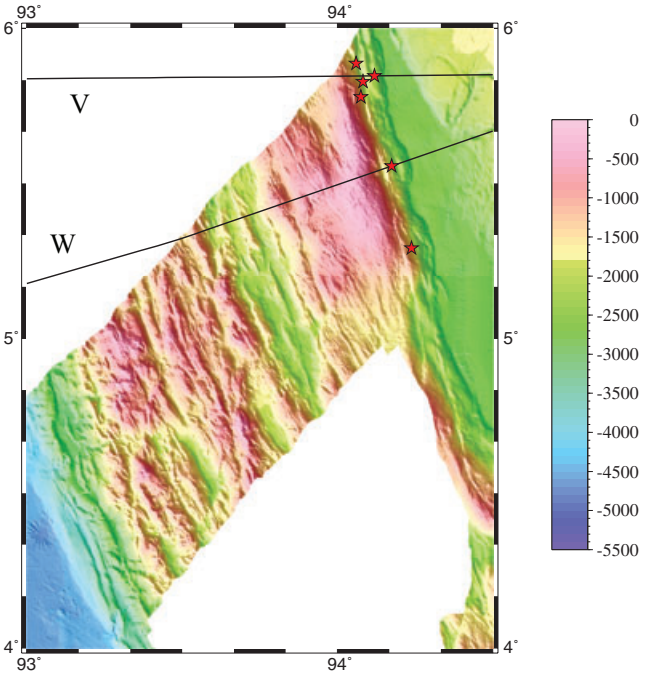

Figure 11. Shaded relief map of swath bathymetry collected by *R/V Marion Dufresne* (Sibuet 2005) in a corridor extending across the accretionary prism from undisturbed Indian Ocean sediments in the SW to the Aceh basin in the NE. Bathymetry is illuminated from the SW and the colour scale in metres is shown to the right of the map. Red stars show the location of the West Andaman Fault on shipboard profiles and the black lines show ship tracks for profiles V and W shown in Fig. 5.

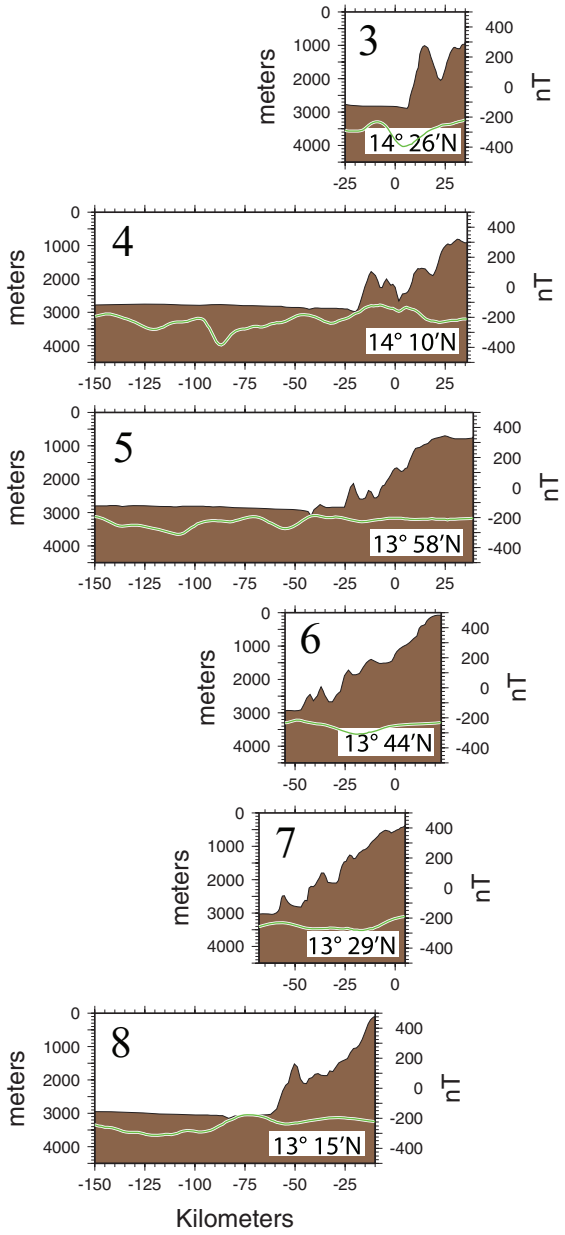

Figure 12. Shipboard geophysical profiles across the trench and onto the accretionary prism between 13°N and 14° 30′N. Numbers on the profiles correspond to those on Fig. 4, which shows the ship tracks for each profile. Bathymetry is in brown and total intensity magnetic anomalies are in green. Profiles are projected along an east–west line with west to the left. The origin for each profile is at 92°30′E and the latitude at 92°30′E is noted. Vertical exaggeration is 16.67:1.

scarp) can be traced continuously to 9°55′N (Figs 4 and 6, profile M), ∼45 km south of the Andaman spreading centre axis. Here, the east scarp of the ridge is a fault called F3 by Kamesh Raju *et al.* (2004).

The WAF extends parallel to the West Sewell Ridge from just NE of Great Nicobar Island to the Andaman spreading centre (Figs 4 and 6, profiles M–Q). It can be traced north of the spreading centre to the base of the Myanmar continental rise (Figs 4 and 6, profile L, Fig. 7). In this region, the WAF passes just to the west of the volcanic Barren and Narcondam Islands. There is no bathymetric or potential field evidence of its presence along strike beneath the Myanmar shelf (Fig. 8, profiles D, E).

A sharp east-facing scarp, often with several thousand metres of relief, characterizes the WAF throughout its entire length (Figs 6 and 7). It is the most prominent bathymetric feature of the Andaman Sea and, particularly south of 12°N, serves to divide the sea between a shallower western forearc region and a deeper eastern backarc basin. From its intersection with the spreading centre at 10°45′N northwards to about 12°, the WAF scarp forms the eastern margin of Invisible Bank, which reaches to within a few metres of the sea surface north of 11°N (Fig. 6, profile L, and Fig. 7, profiles J, K).

The WAF marks the eastern boundary of the forearc basin from 8°30′N to the Myanmar shelf (Figs 4, 6 and 7). In this region, it also forms the eastern boundary of a deep gravity low over the forearc basin (Figs 6, 7 and 10). South of 8° 30′N to 7°N, there is no forearc basin and the WAF is the eastern boundary of the outerarc ridge, the boundary between the forearc and backarc regions and perhaps also the principal boundary between the Sunda Plate and the Burma sliver plate. South of 7°N, the WAF cuts into the forearc area and continues south offshore of Sumatra with one of the strands of the Sumatran fault system becoming the primary boundary between the stable Sunda Plate and the deforming sliver plate. In this region, the WAF is the boundary between the outerarc ridge and the Aceh forearc basin (Figs 4, 5 and 14).

The Eastern Margin Fault (EMF) forms the boundary between the outerarc ridge and a forearc basin to the east of Little Andaman and Car Nicobar Islands (Fig. 6, profiles J, K, Fig. 5, profiles L–P, and Fig. 9a,b). The fault can be traced from about 8°30′N to just north of 11°N (Fig. 4). It is well developed on the northernmost available profile (Fig. 6, profile J) and undoubtedly continues north to the sharp offset in the bathymetry near 11°40′N (Fig. 4). Throughout this region, the EMF coincides with a steep gravity gradient forming

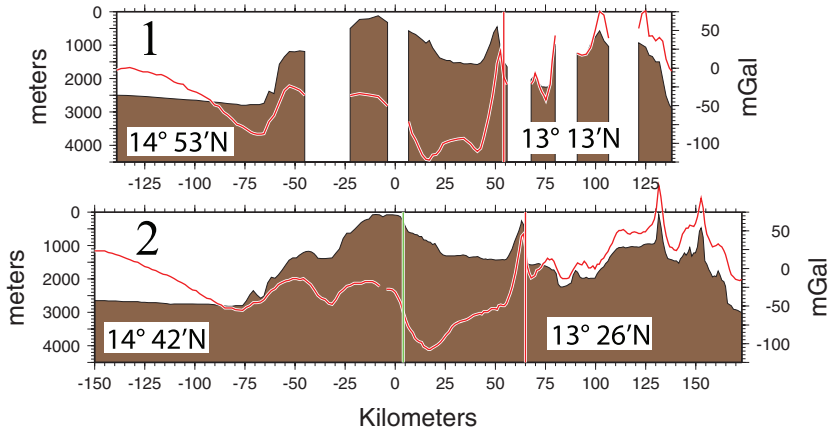

Figure 13. Shipboard geophysical profiles from the Andaman Sea across the accretionary prism near 15°N. Numbers on the profiles correspond to those on Fig. 4, which shows the ship tracks for each profile. Bathymetry is in brown and free-air gravity anomalies are in red. Profiles are projected along an east–west line with west to the left. The origin for each profile is at 93°30′E. Red vertical lines show the location of the West Andaman Fault and the green vertical line shows the location of a possible northern equivalent to the Eastern Margin Fault. The latitude at which each profiles crosses the WAF is noted on the right and the latitude at the base of the accretionary prism is noted on the left. Vertical exaggeration is 16.67:1.

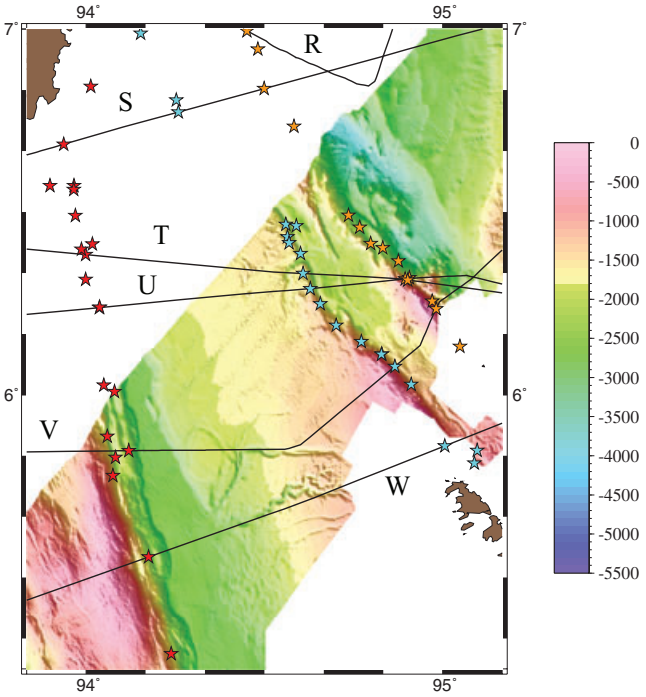

Figure 14. Shaded relief map of swath bathymetry collected by *R/V Marion Dufresne* (Sibuet 2005) across the Aceh Basin and Sumatran Fault System. Bathymetry is illuminated from the SW and the colour scale in metres is shown to the right of the map. Stars show the location of the West Andaman Fault (red), and the Aceh (teal) and Seulimeum (orange) strands of the Sumatran Fault System on shipboard profiles. Black lines show ship tracks for profiles shown in Fig. 5.

the western edge of the deep gravity low over the foreland basin (Fig. 6, profiles N, O, Fig. 7, profile K, and Fig. 10).

A steep bathymetric slope observed on three bathymetric profiles located farther north between 12°05′N and 12°28′N (Fig. 4) could be interpreted as an equivalent feature to the EMF. However this is probably not the case since the gravity gradient forming the western edge of the forearc gravity low is clearly farther to the west on profiles H and I (Fig. 7).

There is only a meager amount of data available from the forearc basin north of 12°30′N (Fig. 3). The satellite altimetry-derived bathymetry map (Smith & Sandwell 1997) shows a very steep slope between the accretionary prism and the forearc basin (Fig. 4). The only available shipboard profiles from the basin onto the Andaman Ridge are located near 14°18′N in the extreme NW corner of the basin (Fig. 13). A scarp coincides with the western gravity gradient in one of these profiles (there is a data gap at the location on the other profile). Thus, a northern equivalent of the EMF is shown to be present in Fig. 4 from 13°N to 14°20′N where the eastern edge of the accretionary prism appears very steep and the gravity low is well developed (Figs 4 and 9).

The Diligent Fault extends through the forearc basin south of 11°40′N. North of about 9°30′N, the fault divides the basin into a shallower western portion at depths of 1250–1500 m and a deeper eastern portion at 2500–3000 m (Fig. 7, profiles J, K, and Fig. 6, profiles L, M). South of 9°30′, the eastern part of the basin shallows and the morphology becomes more complicated (Fig. 6, profiles N–P).

The tectonic diagram of Curray (2005) shows the Diligent Fault extending through West Basin to the Myanmar shelf and he suggests that it may continue north across the shelf to join the Kabaw fault. Since he has no shipboard data across the assumed extension of the Diligent Fault through West Basin, the basis of this hypothesis is unclear. In the two profiles shown in Fig. 13, which were not available to Curray (2005), there is a steep slope near 14°N southeast of the scarp that I identified as a possible northern equivalent of the EMF. There is also an ∼800 m scarp present near the western end of a seismic line across the forearc basin at 13°N shown by Kamesh Raju *et al.* (2007). Stars on Fig. 4 note these locations. However there is simply insufficient data from the northern basin to interpolate between them or to determine whether those scarps are part of a feature equivalent to the Diligent Fault.

5.1 WAF and the Sumatran Fault system

The shallow earthquakes shown in Fig. 2(a) define the current boundary between the stable Sunda Plate and the deforming Burma sliver plate. This boundary extends through Sumatra along the Sumatran fault system and then along the WAF and West Sewell

Ridge to the Andaman spreading centre, along the spreading centre and then through East Basin towards the Sagaing Fault in Myanmar. The earthquake locations are not well enough constrained, even after application of the EHB relocation technique by Engdahl *et al.* (2007), to determine whether the WAF or the Seulimeum fault forms the plate boundary or if the motion is somehow partitioned between the two faults (Fig. 2a).

In Sumatra, Sieh & Natawidjaja (2000) conclude that the Aceh strand of the Sumatran Fault System, which appears to merge with the WAF to the east of Nicobar, is presently inactive. Matson & Moore (1992) and Sieh & Natawidjaja (2000) argue that the Aceh strand absorbed most of the trench parallel component of motion until 2 Ma. Trench-parallel motion was then partitioned between the two faults with the Aceh initially carrying the larger share. However Sieh & Natawidjaja (2000) conclude that the Seulimeum strand is now the primary active fault and that there is no evidence of motion on the Aceh strand for the past 100 ka. This implies that the WAF/Aceh system was the primary plate boundary in the southern Andaman Sea, but that the boundary has recently stepped eastward to the Seulimeum strand.

This scenario is compatible with the bathymetry of the southern Andaman Sea where the WAF forms the main morphologic boundary between the forearc and backarc regions and is paralleled on the east by the West Sewell Ridge (Figs 4 and 6, profiles M–Q). However, there are complications at the intersection of these ridges with the Andaman spreading centre. The Andaman spreading centre consists of three segments (Kamesh Raju *et al.* 2004) (Figs 1 and 4). The eastern segment, to the east of 94°21′E, is marked by a sediment-floored rift valley within a relatively flat sedimented plain. There are no recognizable magnetic seafloor spreading anomalies over the eastern segment (Curray *et al.* 1979; Kamesh Raju *et al.* 2004), which is a common observation at heavily sedimented spreading centres (e.g. Larson *et al.* 1972; Levi & Riddihough 1986; Fukuma & Shinjoe 1998; Gee *et al.* 2001). The central segment is less sedimented and magnetic anomalies are present. Kamesh Raju *et al.* (2004) identified a sequence from the axis to Anomaly 2a (∼3 Ma, Cande & Kent 1995; Gradstein *et al.* 2004) and concluded that seafloor spreading began at about 4 Ma. Only the axial anomaly is present in the western segment and this anomaly narrows to the west, suggesting that the ridge axis has propagated towards the WAF within the past 700 ka (Kamesh Raju *et al.* 2004).

The boundary between the western and central spreading segments is directly north of the valley to the east of the West Sewell Ridge. This suggests that the plate boundary was the Seulimeum strand along the eastern edge of the West Sewell Ridge prior to 700 ka, but may have recently shifted to the WAF. This is the reverse of what is suggested by the tectonic relationships in northern Sumatra. One solution to this conundrum is that the active Seulimeun strand did continue north to the spreading centre, but that coincident with the westward propagation of the spreading centre towards the WAF, the Seulimeun strand linked with the WAF near 9°30′N as suggested by Curray (2005).

The WAF continues north of the Andaman spreading centre and can be traced continuously to the Myanmar shelf (Fig. 4). It passes just west of the Barren Island and Narcondam Island volcanoes and swings to the east as it approaches the continental rise. There is no sign of its presence in the available geophysical profiles on the shelf (Fig. 8, profiles D, E). Curray (2005) considers the ridge that I have associated with the WAF north of about 13°N (e.g. Fig. 7, profile F, and Fig. 13, profiles 1, 2) to be a different feature that he calls the Cocos Fault and suggests may be a splay off of his hypothesized extension of the Diligent Fault through West Basin. However, the fact that those crossings are directly along the trend established by the WAF to the south, have the same morphologic form as the WAF and, like the WAF, form the eastern edge of the forearc gravity low (Fig. 10) lead me to identify them as the WAF.

The WAF remains a prominent morphologic feature to the north of the Andaman spreading centre and probably was one of the primary active structures prior to the initiation of the spreading centre. As is the case to the south of the spreading centre, a gravity high over the WAF forms the eastern boundary of the deep gravity low over the forearc basin (Fig. 7, profiles H, I, K, and Fig. 10). Its probable role as a (perhaps now fossil) plate boundary is also suggested by the observation that it passes close to the Barren Island and Narcondam Island volcanoes in the same manner that the Sumatran fault follows the volcanic arc in Sumatra (although Sieh & Natawidjaja (2000) argue that the association of the fault and volcanic arc in Sumatra is coincidental). The northern portion of the WAF may well have remained active during the early stages of seafloor spreading when the spreading rate was lower than at present (Kamesh Raju *et al.* 2004). It is not apparent whether there is currently any active strike slip motion on the northern WAF. A number of shallow earthquake epicentres are located near the northern WAF (Fig. 2a), but it not possible to assign them to the WAF with any confidence.

The WAF has a characteristic morphologic expression to the north of about 8° 30′N. On most of the bathymetry profiles, it is associated with a bathymetric ridge that has a very sharp eastern flank and gentler western flank (Figs 6, 7, 9a and b). Curray (2005) argued that the WAF ridge north of about 9°N is a cuesta formed by a component of compression and uplift across the fault. In particular, Curray (2005) suggested that the very shallow depth of Invisible Bank resulted from post-Miocene uplift due to compression and reverse faulting resulting from seafloor spreading at the Andaman spreading centre. This is supported by a dredge sample recovered from a depth of 490 m at 11°51′N (a few km south of profile I on Fig. 7) that contained a late Miocene (Zone N17) fossil assemblage that included benthic foraminifera normally found deeper than 1000 m (Frerichs 1971).

5.2 The Eastern Margin and Diligent Faults

The Eastern Margin Fault is a major down-to-the-east fault that marks the boundary between the outerarc ridge and a forearc basin from 8°30′N to 11°40′N (Figs 6 and 7, profiles J and K). The fault also coincides with a steep gravity gradient, which forms the western flank of the gravity low over the forearc basin (Fig. 6, profiles N and O, Fig. 7, profile K, and Fig. 10).

Based on satellite altimetry derived bathymetry (Fig. 4) and free-air gravity anomalies (Fig. 10), an equivalent fault appears to be present east of North Andaman Island extending north to the Myanmar shelf. However there are no shipboard data to confirm that assumption or to characterize the hypothesized fault.

The WAF south of Nicobar Island occupies a similar position to that of the Eastern Margin Fault further north. Specifically, it marks an abrupt eastern boundary to the outerarc ridge and forms the western edge of the Aceh forearc Basin (Figs 4 and 5). However, the tectonic setting of this southern portion of the WAF is somewhat different than that of the Eastern Margin Fault. The WAF south of 7°N, where it cuts across the forearc and bounds the Aceh Basin is an active strike slip fault (e.g. Seeber *et al.* 2007; Sibuet *et al.* 2007; Berglar *et al.* 2010) and has played an important role in the development of the Sumatran forearc region (e.g. Curray *et al.* 1979; Izart *et al.* 1994; Samuel *et al.* 1997; Sieh & Natawidjaja

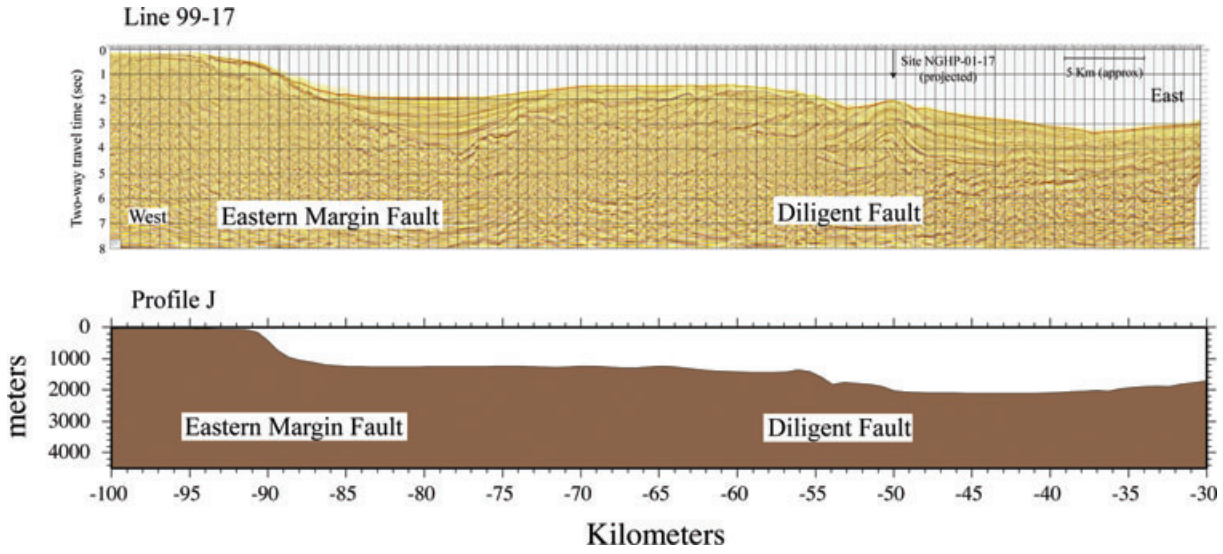

Figure 15. Multichannel seismic reflection line from just east of Little Andaman Island to the lower slope of Invisible Bank. The line was run W–E near 10° 38′N, ∼13 km south of Site NGHP-01-17 and its location is shown on Fig. 4. It is located roughly midway between profile L (Fig. 6) and profile J (Fig. 7). Vertical exaggeration is ∼2:1. Nearby bathymetric profile J (Fig. 7) is also shown at the same vertical exaggeration to demonstrate the effect of different vertical exaggerations on the appearance of the bathymetric features.

2000; Curray 2005). On the other hand, it is unlikely that the Eastern Margin Fault has experienced strike slip motion. It has a finite length and is bounded by structures that show no evidence of strike slip deformation (Fig. 4). It thus appears to have experienced exclusively dip slip motion. This difference in tectonic history may account for the unusual nature of the Diligent Fault, which has no counterpart in the Aceh forearc basin.

The Diligent Fault runs through the entire length of the forearc basin bounded by the Eastern Margin Fault. North of about 9°30′N, it has a significant vertical offset and divides the basin into a shallow western part at 1250–1500 m depth and a deeper eastern part at 2500–3000 m depth (Fig. 6, profiles L and M, Fig. 7, profiles J and K, and Fig. 9a). South of 9°30′N, this division no longer exists as offset on the Diligent Fault greatly decreases and the eastern part of the basin shoals to about 1500 m. However, a feature that appears to be the Diligent Fault can be traced continuously along strike (Figs 4 and 6, profiles N–P, and Fig. 9b). Curray (2005) characterizes the Diligent Fault as primarily a normal fault that may have also experienced some strike slip motion.

Fig. 15 shows a regional west to east multichannel seismic reflection line (line 99–17) from an oil industry survey that served as the site survey for Site NGHP-01-17 (Collett *et al.* 2008a,b). The seismic line is located at ∼10°38′N, ∼13 km south of Site NGHP-01-17 and its location is shown on Fig. 4. It is located roughly midway between profile L (Fig. 6) and profile J (Fig. 7). The line extends from the shelf east of Little Andaman Island across the Eastern Margin and Diligent Faults onto the lower slope of Invisible Bank. Fig. 16 shows enlargements of portions of the seismic line crossing the EMF and the Diligent Fault.

The Diligent Fault in Line 99–17 does not appear to be as prominent a feature as in the crossings of the fault shown in Figs 6, 7 and 9. In fact there is 1400 m (1.85 s twtt) relief across it on the seismic line. The difference in appearance is completely the result of the vertical exaggeration in the various figures. The vertical exaggeration in Figs 15 and 16 is approximately 2:1. The vertical exaggeration is 16.67:1 for the bathymetric profiles shown in Figs 6 and 7, and is 30:1 for the analogue seismic sections shown in Fig 9. The portion of nearby profile J (Fig. 7) crossing the EMF and the Diligent Fault is also shown in Fig. 15 with a 2:1 vertical exaggeration to illustrate the effects of changing the vertical exaggeration.

The low vertical exaggeration allows the subsurface structure to be clearly displayed. The Eastern Margin Fault (EMF) is a down to the east normal fault (Fig. 16a). The footwall of the fault can be traced to a depth of about 2 s twtt beneath undisturbed sediments that form a basin roughly 10 km wide. Sediment packages thicken towards the centre of the basin suggesting continuing subsidence and motion on the EMF. This is also suggested by the observation that the region of the basin forms a 400 m (∼0.5 s twtt) depression of the seafloor. A similar depression can be observed on almost all of the profiles across the EMF (Figs 6, 7, 9a and b).

On the eastern side, the sediments filling the basin at the foot of the EMF lap up onto a crumpled mass of sediments that form the hanging wall of the fault. These sediments are disturbed and display compressional deformation that appears to increase towards the Diligent Fault (Fig. 15). Immediately to the west of the projection of Site NGHP-01-17, thrusting can be observed within the sedimentary section with slices stacked on each other (Fig. 16b). The deformation reaches to the seafloor in places. Site NGHP-01-17 is located at the crest of an anticlinal feature that produces positive relief on the seafloor. Sediments lap up onto both flanks of the anticline suggesting recent and probably continuing relative uplift. The sedimentary section to the east of the anticline, filling the deepest portion of the forearc basin and forming the west flank of Invisible Bank appears to be undeformed. Deformed sediments are also present between the EMF and the Diligent Fault on the seismic sections in Figs 9(a) and (b), but the very high vertical exaggeration on those analogue lines prevents determination of any details. These observations suggest that the Diligent 'Fault' is actually a deformation front and the Diligent Fault anticline may have developed above an eastward vergent blind thrust bounding the deforming portion of the hanging wall on the downdip side.

The structure observed on Line 99–17 raises the question of how and why these compressive structures formed. A related question is simply how did the forearc basin, bounded on the west by a large normal fault (the EMF) form within what is basically a compressive tectonic environment. The basin is situated east of the accretionary

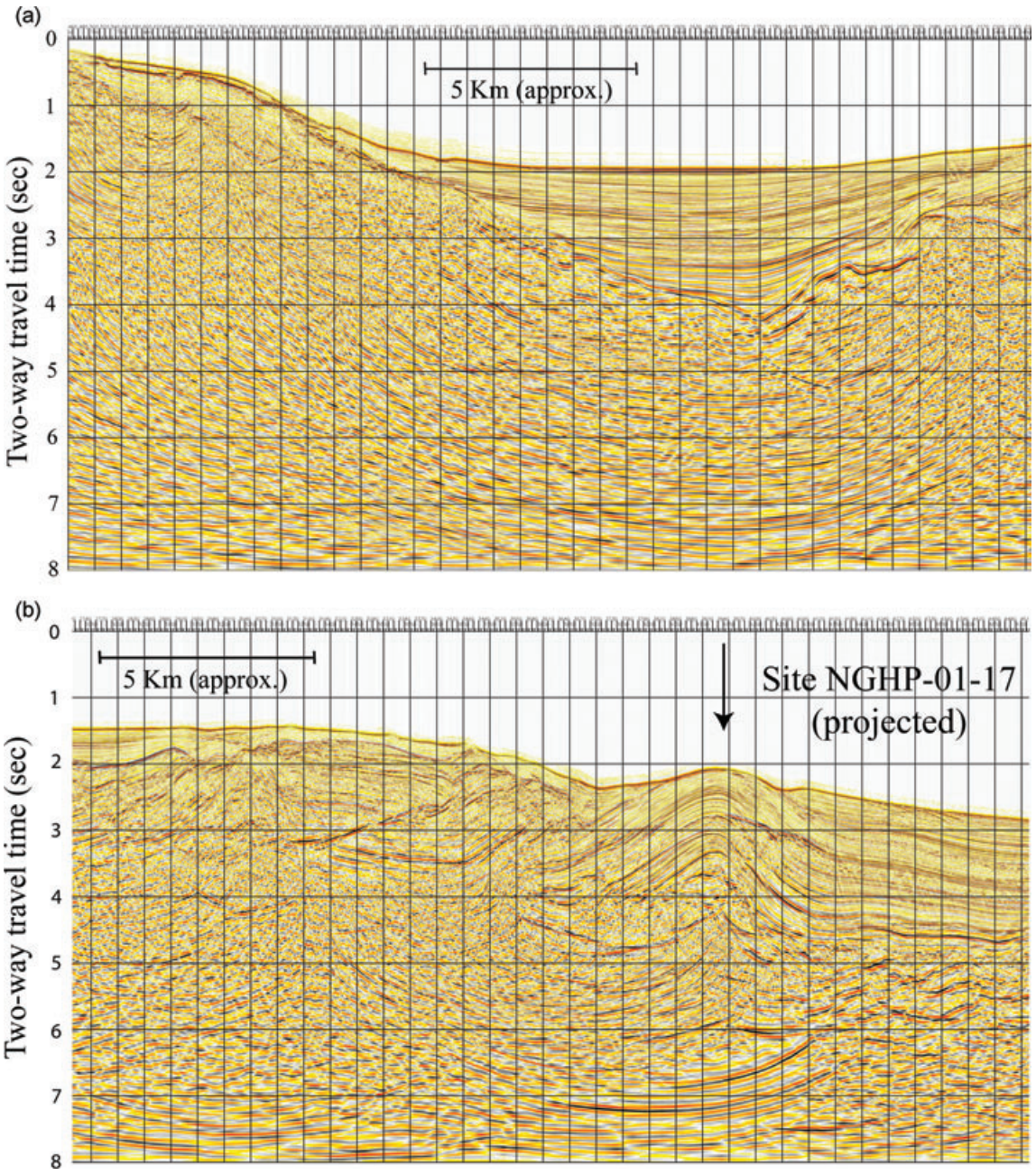

Figure 16. Detail of the seismic line shown in Fig. 15 showing the region of: (a) the Eastern Margin Fault (EMF). Note the incompletely filled basin overlying the fault, suggesting continuing motion, and the disturbed nature of the sediments making up the hanging wall. Vertical ruling is at 50 CDP (common depth point) intervals or ∼625 m and (b) the Diligent 'Fault' anticline and the compressional deformation to the west of the anticline. Vertical ruling is at 50 CDP (common depth point) intervals or ∼625 m. Vertical exaggeration is ∼2:1.

prism, which has developed as the result of west to east directed compression of the off-scraped sediments. It is also immediately to the west of Invisible Bank which formed as the result of an east to west directed component of compression across the WAF (Curray 2005).

A possible answer is that the forearc basin did not form by east–west crustal extension, but rather as the result of subduction erosion of the crust from below. A possible analogue is the Aleutian Terrace, which runs nearly the entire length of the Aleutian forearc and is underlain by a forearc basin that has been attributed to subduction erosion (Ryan & Scholl 1995; Scholl *et al.* 2002, 2006; Clift & Vannucchi 2004). As is the case with the Andaman forearc basin, the Aleutian forearc basin is separated from the accretionary complex by a structural high (outerarc ridge) and is bounded on its trenchward side by normal faults (e.g. Grow 1973; Harbert *et al.* 1986; Scholl *et al.* 1987; Ryan & Scholl 1989). The Aleutian outerarc ridge and forearc basin are underlain by arc basement (Ryan & Scholl 1989) [also see seismic sections published by Holbrook *et al.* (1999), Fliedner & Klemperer (2000) and Lizarralde *et al.* (2002)]. The Aleutian forearc basin developed by rapid subsidence beginning in the latest Miocene (Scholl *et al.* 1987) that Ryan & Scholl (1995) and Scholl *et al.* (2002, 2006) ascribe to crustal thinning as the result of subduction erosion. Scholl *et al.* (2002) argue that a sharp increase in sediment input to the trench in the Late Miocene

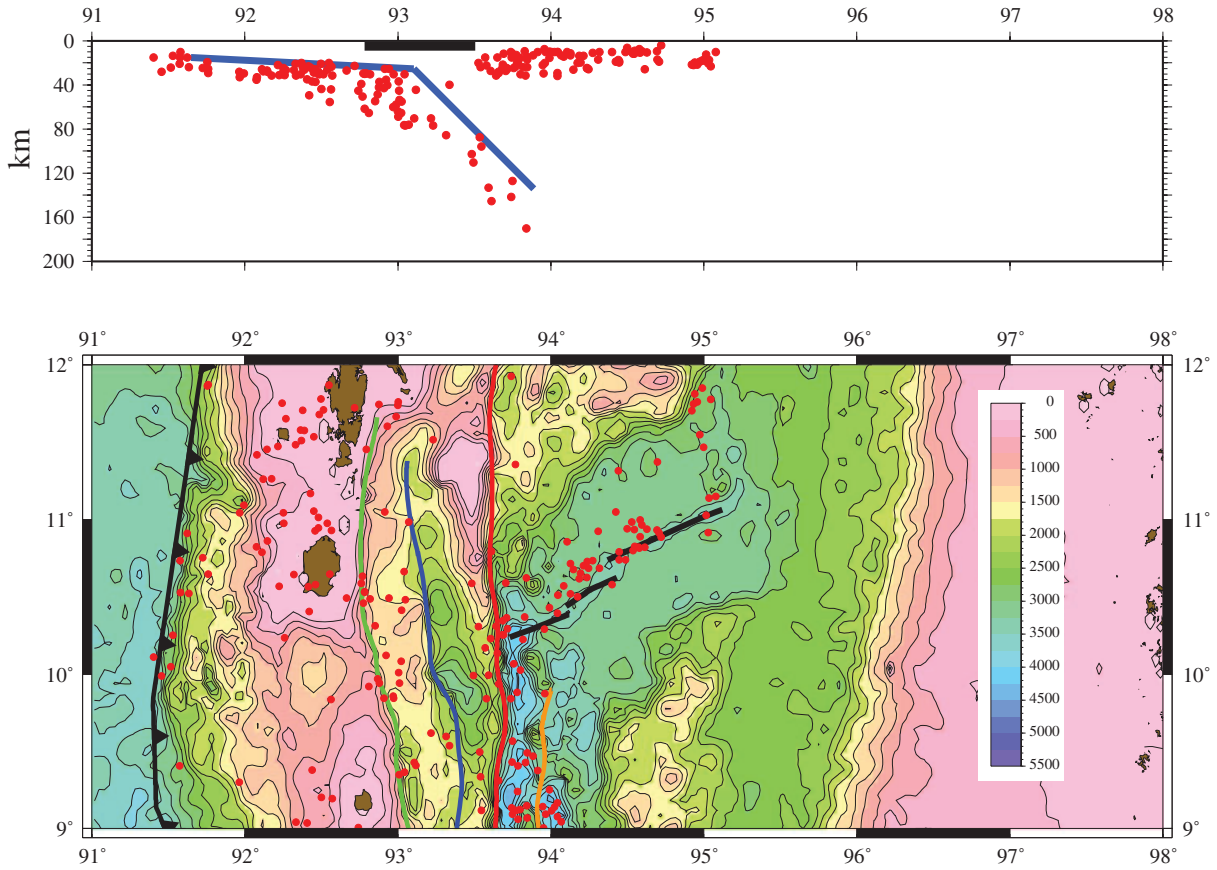

Figure 17. Location of earthquakes in the Andaman Sea between 9°N and 12°N relocated using the EHB technique and for which the depth is noted as 'reviewed and accepted' by Engdahl *et al.* (2007). A map view is shown on the bottom and a cross section on the top. In the map view, bathymetry is derived from satellite altimetry (Smith & Sandwell 1997) and is contoured at 250 m intervals. Insert gives bathymetric colour scale in metres. The trace of the EMF is shown in green, the Diligent Fault in blue, the WAF in red and the Seulimeum strand in orange. The locations of the Andaman spreading centre and the Sunda Trench are shown in black. The heavy black line at the top of the cross-section shows the east–west extent of the forearc basin. Location of the top of the subducting slab, estimated from the earthquake locations, is shown as a blue line.

(McCarthy & Scholl 1985) resulted in increasing the amount of sediment subducted along the nearly horizontal subduction zone even as an accretionary prism was developing. Subduction of water-rich sediment can result in the development of overpressures causing hydrofracturing and dislodgement of blocks of the upper plate (e.g. von Huene *et al.* 2004). Scholl *et al.* (2002) point out that the axis of the forearc basin is at the inner edge of the flat portion of the slab where it bends sharply down. This is also the case with the Andaman forearc basin (Fig. 17). The Indian Plate lithospheric slab extends at a shallow angle beneath the accretionary prism and Andaman Nicobar Ridge and then turns sharply down beneath the forearc basin. A number of studies have observed that great subduction zone earthquakes systematically occur beneath forearc basins (Nishenko & McCann 1979; Song & Simons 2003; Wells *et al.* 2003; Rosenau & Oncken 2009). This observation implies significant coupling and interaction between the plates beneath the forearc basin. This coupling could result in formation of the basin by crustal thinning from below.

The nature of the crust under the Andaman forearc basin is not known (Curray 2005), basically for lack of data. Further south, to the west of Sumatra, Kieckhefer *et al.* (1980) found that the forearc basin east of Nias Island is underlain by a 20-km thick layer of material with a *P*-wave velocity of 6.5–6.8 km s^{-1}. Similarly Singh *et al.* (2008) identified subhorizontal reflectors on a multichannel seismic reflection line that they identified as continental Moho at 20–25 km depth below the Simeulue forearc basin. Clearly the geological setting of the Andaman forearc basins is somewhat different since they are located west of the Andaman Sea rather than west of Sumatra. However, if they are underlain by arc crust or continental crust remaining from the pre-subduction margin, then subduction erosion, thinning this crust and resulting in subsidence is a possible mechanism to create the basin in the absence of east–west extension.

6 SUMMARY AND CONCLUSIONS

The Andaman forearc has developed as the result of highly oblique subduction at the western Sunda Trench, leading to partitioning of convergence into trench-perpendicular and trench-parallel components. The principal elements of the Andaman forearc are the Andaman–Nicobar Ridge, which is the accretionary prism and outerarc ridge of the subduction zone, and a series of forearc basins that bound the Andaman–Nicobar Ridge to the east. Several major N–S faults have played important roles in the development of the forearc region to the east of the Andaman–Nicobar Ridge.

The Andaman–Nicobar Ridge is an imbricate stack of fault slices and folds consisting of slivers of seafloor ophiolites and the overlying sediments, capped by Neogene shallow water sediments. The western, outer slope of the accretionary prism is very steep, rising

from the level of the Bengal Fan sediments to a terrace at a depth of 1500–2000 m within a distance of 30 km. The eastern edge of the Andaman–Nicobar Ridge is fault bounded and, north of the Nicobar Islands, a forearc basin is located between the ridge and the WAF. A deep gravity low with very steep gradients lies directly over the forearc Basin.

There is a distinct difference in the nature of the short wavelength morphology between the western and eastern portions of the accretionary prism. The outer portion is characterized by a series of short-wavelength anticlines and synclines with amplitudes of a few hundred to about one thousand m resulting from ongoing deformation of the sediments. The inner portion is smoother with lower slopes (Fig. 11). Near 5°N, the boundary between these two regions may correspond to a major seaward verging thrust (Sibuet *et al.* 2007; Lin *et al.* 2009) that separates the prism into a deforming outer portion and a stronger inner backstop. The width of the outer deforming portion of the accretionary prism, which is 80–100 km south of 10°N, narrows to about 40 km between 10°N and 11°30′N. It remains at about 40 km to ∼14°40′N. North of there, the inner trench wall becomes a single steep slope up to the Myanmar shelf. These changes in the width of the accretionary prism correspond to variations in the trench-perpendicular component of motion between the Indian and Sunda plates (Socquet *et al.* 2006). The change to a single steep slope occurs near the northern end of the rupture zone of the great 2004 December 26 earthquake.

The morphology and tectonics of the eastern portion of the Andaman forearc is controlled by a number of major north–south trending faults. The WAF and the Seulimeum strand of the Sumatra Fault System (along the east flank of the West Sewell Ridge) form the boundary between the Sunda Plate and the deforming Burma Plate to the south of the Andaman spreading centre (Fig. 4). The spreading centre has recently propagated from the Seulimeum Fault to the WAF and it is not clear which fault is active plate boundary or whether motion is somehow partitioned between them. The Seulimeum strand is the principal active fault in northern Sumatra (Sieh & Natawidjaja 2000). The WAF can be traced north of its intersection with the spreading centre to the Myanmar shelf. This portion of the fault passes just west of the volcanic Barren and Narcondam Islands and appears to have been one of the primary active tectonic structures prior to the initiation of seafloor spreading at ∼4 Ma.

The WAF is the most prominent morphologic feature of the Andaman Sea. South of 12°N, it divides the Andaman Sea into a shallow forearc and a deeper backarc region. From 8°N north to the Myanmar shelf, the WAF forms the eastern boundary of a set of forearc basins (Figs 4–7). The Eastern Margin Fault forms the boundary between the Andaman–Nicobar Ridge and the forearc basin from 8°30′N to 11°40′N. An equivalent fault plays the same role from about 12°30′N to the Myanmar shelf. These faults appear to have experienced primarily dip slip motion. These two faults and the WAF to the east bound a deep free-air gravity low over the forearc basin (Fig. 10).

The Diligent fault runs through the forearc basin from 8°30′N to 11°N (Figs 4 and 6). The Diligent Fault has the appearance a normal fault on high vertical exaggeration bathymetric profiles and the previously available analogue single-channel seismic reflection profiles. However, oil industry multichannel seismic reflection data show it to be associated with compressive deformation. Site NGHP-01-17 is located at the crest of an anticlinal feature that produces positive relief on the seafloor. Sediments lap up onto both flanks of the anticline suggesting recent relative uplift. Farther west, thrusting can be observed within the sedimentary section (Fig. 16b) and this deformation reaches to the seafloor. The Diligent 'Fault' may actually be a deformation front separating deforming sediments of the hanging wall of the Eastern Margin Fault from undeformed sediments to the east. This could result if the forearc basin did not form through east–west extension but rather as the result of crustal thinning from below through subduction erosion, which results in subsidence but produces limited accommodation space for the hanging wall of the EMF.

ACKNOWLEDGMENTS

I thank Tim Collett and Dave Goldberg for inviting me to participate in NGHP Expedition 01. I thank Professor Joe Curray and Dr K.A. Kamesh Raju for useful discussions and for providing me with copies of their published seismic lines in a usable scale and format. Giles Guerin assisted with the preparation of the seismic line shown in Figs 15 and 16. Joe Curray and Tim Henstock provided valuable comments and criticisms. The GMT software package (Wessel & Smith 1998) was used extensively in data analysis and the preparation of figures. This work was supported by the United States Geological Survey. LDEO contribution 7367.

REFERENCES

Ammon, C.J., *et al*. 2005. Rupture process of the 2004 Sumatra-Andaman earthquake, *Science,* **308,** 1133–1139.

Bellier, O. & Sebier, M., 1995. Is the slip rate variation on the Great Sumatran Fault accommodated by fore-arc stretching? *Geophys. Res. Lett.,* **22,** 1969–1972

Berglar, K., Gaedicke, C., Franke, D., Ladage, S., Klingelhofer, F. & Djajadihardja, Y.S., 2010. Structural evolution and strike-slip tectonics off north-western Sumatra, *Tectonophysics,* **480,** 119–132.

Bilham, R., 2005. A flying start, then a slow slip, *Science,* **308,** 1126–1127.

Bock, Y., Prawirodirdjo, L., Genrich, J.F., Stevens, C.W., McCaffrey, R., Subarya, C., Puntodewo, S.S.O. & Calais, E., 2003. Crustal motions in Indonesia from Global Positioning System measurements, *J. geophys. Res.,* **108,** doi:10.1029/2001/JB000324.

Cande, S.C. & Kent, D.V., 1995. Revised calibration of the geomagnetic polarity timescale for the Late Cretaceous and Cenozoic, *J. geophys. Res.,* **100,** 6093–6095.

Clift, P.D. & Vannucchi, P., 2004. Controls on tectonic accretion versus erosion in subduction zones: implications for the origin and recycling of the continental crust, *Rev. Geophys.,* **42,** RG2001, doi:10.1029/2003RG000127.

Collett, T.S., Riedel, M., Cochran, J.R., Boswell, R., Kumar, P. & Sathe, A.V., 2008a. Indian continental gas hydrate prospects: results of the Indian National Gas Hydrate Program (NGHP) Expedition 01, in *Proceedings of the 6th International Conference on Gas Hydrates (ICGH 2008)*, Vancouver, B.C., Canada, July 6–10, 2008, available at: https://circle.ubc.ca/handle/1429/1035.

Collett, T.S., *et al.* and the NGHP Expedition 01 Scientific Party, 2008b. *Indian National Gas Hydrate Program Expedition 01 Initial Reports,* Prepared by the U.S. Geological Survey and Published by the Directorate General of Hydrocarbons, Ministry of Petroleum and Natural Gas (India), 1 DVD.

Curray, J.R., 2005. Tectonics and history of the Andaman Sea region, *J. Asian Earth Sci.,* **25,** 187–232.

Curray, J.R., Moore, D.G., Lawver, L.A., Emmel, F.J., Raitt, R.W., Henry, M. & Kieckhefer, R., 1979. Tectonics of the Andaman Sea and Burma, in *Geological and Geophysical Investigations of Continental Margins,* pp. 189–198, eds Watkins, J.S., Montadert, L. & Dickerson, P.W., Amer. Assoc. Petrol. Geol. Memoir 29.

Diament, M., *et al*. 1992. Mentawai fault zone off Sumatra: a new key to the geodynamics of western Indonesia, *Geology,* **20,** 259–262.

Engdahl, E.R., Villasenor, A., DeShon, H.R. & Thurber, C.H., 2007. Teleseismic relocation and assessment of seismicity (1918–2005) in the region of the 2004 M_w 9.0 Sumatra-Andaman and 2005 M_w 8.6 Nias Island great earthquakes, *Bull. seism. Soc. Am.,* **97,** S43-S61.

Fisher, D., Mosher, D., Austin, J.A., Gulick, S.P.S., Masterlark, T. & Moran, K., 2007. Active deformation across the Sumatran forearc over the December 2004 M_w 9.2 rupture, *Geology,* **35,** 99–102.

Fitch, T.J., 1972. Plate convergence, transcurrent faults and internal deformation adjacent to Southeast Asia and the western Pacific, *J. geophys. Res.,* **77,** 4432–4460.

Fliedner, M.M. & Klemperer, S.L., 2000. Crustal structure transition from oceanic arc to continental arc, Eastern Aleutian Islands and Alaska Peninsula, *Earth planet. Sci. Lett.,* **179,** 567–579.

Frerichs, W.E., 1971. Paleobathymetric trends for Neogene formaminiferal assemblages and sea floor tectonism in the Andaman Sea area, *Mar. Geol.,* **11,** 153–173.

Fukuma, K. & Shinjoe, H., 1998. Origin of the absence of magnetic anomalies in the Yamato Basin of the Japan Sea: magnetic properties of mafic rocks from Ocean Drilling Program Hole 794D, *J. geophys. Res.,* **103,** 17 791–17 805.

Gee, J.S., Webb, S.C., Ridgway, J., Staudigel, H. & Zumberge, M.A., 2001. A deep tow magnetic survey of Middle Valley, Juan de Fuca Ridge, *Geochem. Geophys. Geosyst.,* **2,** doi:10.1029/2001GC000170.

Genrich, J.F., Bock, Y., McCaffrey, R., Prawirodirdjo, L., Stevens, C.W., Puntodewo, S.S.O., Subarya, C. & Wdowinski, S., 2000. Distribution of slip at the northern Sumatra fault system, *J. geophys. Res.,* **105,** 28 327–28 341.

Gradstein, F.M., Ogg, J.G. & Smith, A., 2004. *A Geologic Time Scale 2004,* pp. 589, Cambridge University Press, Cambridge.

Graindorge, D., *et al*. 2008. Impact of lower plate structure on upper plate deformation at the NW Sumatran convergent margin from seafloor morphology, *Earth planet. Sci. Lett.,* **275,** 201–210.

Grow, J.A., 1973. Crustal and upper mantle structure of the central Aleutian arc, *Bull. Geol. Soc. Am.,* **84,** 2169–2192.

Guzman-Speziale, M. & Ni, J., 1993. Opening of the Andaman Sea: where is the short-term displacement being taken up? *Geophys. Res. Lett.,* **20,** 2949–2952.

Harbert, W., Scholl, D.W., Vallier, T.L., Stevenson, A.J. & Mann, D.M., 1986. Major evolutionary phases of a forearc basin of the Aleutian terrace: relation to North Pacific tectonic events and the formation of the Aleutian subduction complex, *Geology,* **14,** 757–761.

Henstock, T.J., McNeill, L.C. & Tappin, D.R., 2006. Seafloor morphology of the Sumatran subduction zone: surface rupture during megathrust earthquakes? *Geology,* **34,** 485–488.

Holbrook, W.S., Lizarralde, D., McGeary, S., Bangs, N.L.B. & Diebold, J., 1999. Structure and composition of the Aleutian island arc and implications for continental crustal growth, *Geology,* **27,** 31–34.

Izart, A., Mustafa Kemal, B. & Malod, J.A., 1994. Seismic stratigraphy and subsidence evolution of the northwest Sumatra fore-arc basin, *Mar. Geol.,* **122,** 109–124.

Jarrard, R.D., 1986. Terrane motion by strike-slip faulting of forearc slivers, *Geology,* **14,** 780–783.

Johnson, J.E., Giosan, L., Rose, K. & Fraschetti, J., 2007. Stratigraphy, sedimentology, and depositional history of gas hydrate bearing sediments along the eastern continental margin of India and in the Andaman accretionary wedge: results of NGHP Expedition 01, *EOS, Trans. Am. Geophys.,* **88**(52), Fall. Meet. Supp., Abstract OS11C-02.

Kamesh Raju, K.A., Ramprasad, T., Rao, P.S., Rao, B.R. & Varghese, J., 2004. New insights into the tectonic evolution of the Andaman basin, northeast Indian Ocean, *Earth planet. Sci. Lett.,* **221,** 145–162.

Kamesh Raju, K.A., Murty, G.P.S., Amarnath, D. & Mohan Kumar, M.L., 2007. The West Andaman fault and its influence on the aftershock pattern of the recent megathrust earthquakes in the Andaman-Sumatra region, *Geophys. Res. Lett.,* **34,** L03305, doi:10.1029/2006GL028730.

Kieckhefer, R.M., Shor, G.G., Curray, J.R., Sugiarta, W. & Hehuwat, F., 1980. Seismic refraction studies of the Sunda trench and forearc basin, *J. geophys. Res.,* **85,** 863–889.

Laluraj, C.M., Balachandran, K.K., Sabu, P. & Panampunnayil, S.U., 2006. Persistent volcanic signature observed around Barren Island, Andaman Sea, India, *Mar. Geophys. Res.,* **27,** 283–288.

Larson, P.A., Mudie, J.D. & Larson, R.L., 1972. Magnetic Anomalies and fracture zone trends in the Gulf of California, *Bull. Geol. Soc. Am.,* **83,** 3361–3368.

Lay, T., *et al*. 2005. The great Sumatra-Andaman earthquake of 26 December 2004, *Science,* **308,** 1127–1133.

Levi, S. & Riddihough, R., 1986. Why are marine magnetic anomalies suppressed over sedimented spreading centers? *Geology,* **14,** 651–654.

Lin, J.Y., LePichon, X., Rangin, C., Sibuet, J.C. & Maury, T., 2009. Spatial aftershock distribution of the 26 December 2004 great Sumatra-Andaman earthquake in the northern Sumatra area, *Geochem. Geophys. Geosyst.,* **10,** Q05006, doi:1029/2009GC002454,

Lizarralde, D., Holbrook, W.S., McGeary, S., Bangs, N.L.B. & Diebold, J., 2002. Crustal construction of a volcanic arc, wide-angle seismic results from the western Alaska Peninsula, *J. geophys. Res.,* **107,** (B8), 2164. doi:10.1029/2001JB000230.

Matson, R. & Moore, G., 1992. Structural influences on Neogene subsidence in the central Sumatra fore-arc basin, in *Geology and Geophysics of Continental Margins,* pp. 157–181, eds Watkins, J.S., Zhiqiang, F. & McMillen, K., Am. Assoc. Petrol. Geol., Tulsa, Okla.

McCaffrey, R., 1991. Slip vectors and stretching of the Sumatra fore arc, *Geology,* **19,** 881–884.

McCaffrey, R., 1996. Estimates of modern arc-parallel strain rates in fore arcs, *Geology, **24***, 27–30.

McCaffrey, R., Zwick, P.C., Bock, Y., Prawirodirdjo, L., Genrich, J.F., Stevens, C.W., Puntodewo, S.S.O. & Subarya, C., 2000. Strain partitioning during oblique convergence in northern Sumatra: geodetic and seismologic constraints and numerical modeling, *J. geophys. Res.,* **105,** 28 363–28 376.

McCarthy, J. & Scholl, D.W., 1985. Mechanisms of subduction accretion along the central Aleutian Trench, *Bull. Geol. Soc. Am.,* **96,** 691–701.

Mosher, D.C., Austin, J.A., Fisher, D. & Gulick, S.P.S., 2008. Deformation of the northern Sumatra accretionary prism from high-resolution seismic reflection profiles and ROV observations, *Mar. Geol.,* **252,** 89–99.

Nielsen, C., Chamot-Rooke, N. & Rangin, C., 2004. From partial to full strain partitioning along the Indo-Burmese hyper-oblique subduction, *Mar. Geol.,* **209,** 303–327.

Nishenko, S. & McCann, W., 1979. Large thrust earthquakes and tsunamis: implications for the development of forearc basins, *J. geophys. Res.,* **84,** 573–584.

Pal, T., Chakraborty, P.P., Gupta, T.D. & Singh, C.D., 2003. Geodynamic evolution of the outer-arc-forearc belt of the Andaman Islands, the central part of the Burma-Java subduction complex, *Geol. Mag.,* **140,** 289–307.

Pal, T., Gupta, T.D., Chakraborty, P.P. & Das Gupta, S.C., 2005. Pyroclastic deposits of Mio-Pliocene age in the Arakan-Yoma-Andaman-Java subduction complex, Andaman Islands, Bay of Bengal, India, *Geochem. J.,* **39,** 69–82.

Pal, T., Mitra, S.K., Sengupta, S., Katari, A., Bandopadhyay, P.C. & Bhattacharya, A.K., 2007. Dacite–andesites of Narcondam volcano in the Andaman Sea—an imprint of magma mixing in the inner arc of the Andaman–Java subduction system, *J. Volc. Geotherm. Res.,* **168,** 93–113.

Rodolfo, K.S., 1969. Bathymetry and marine geology of the Andaman Basin and tectonic implications for southeast Asia, *Bull. Geol. Soc. Am.,* **80,** 1203–1230.

Rosenau, M. & Oncken, O., 2009. Fore-arc deformation controls frequency-size distribution of megathrust earthquakes in subduction zones, *J. geophys. Res.,* **114,** B130111, doi:10.1029/2009/2009JB006359.

Ryan, H.F. & Scholl, D.W., 1989. The evolution of forearc structures along an oblique convergent margin, central Aleutian arc, *Tectonics,* **8,** 497–516.

Ryan, H.F. & Scholl, D.W., 1995. Deep reflectors beneath the Aleutian forearc: implications for the geometry of the subducting slab, *EOS, Trans. Am. geophys. Un.,* **76,** F590.

Samuel, M.A., Harbury, N.A., Bakri, A., Banner, F.T. & Hartono, L., 1997. A new stratigraphy for the islands of the Sumatra forearc, Indonesia, *J. Asian Earth Sci.,* **15,** 339–380.

Sandwell, D.T. & Smith, W.H.F., 1997. Marine gravity anomaly from Geosat and ERS1 satellite altimetry, *J. geophys. Res.,* **102,** 10 039–10 054.

Sandwell, D.T. & Smith, W.H.F., 1999. Marine Gravity Anomalies from Satellite Altimetry, Version 9.2 (digital file available by anonymous ftp to baltica.ucsd.edu).

Scholl, D.W., Vallier, T.L. & Stevenson, A.J., 1987. Geologic evolution and petroleum geology of the Aleutian Ridge, in *Geology and Resource Potential of the Continental Margin of Western North America and Adjacent Ocean Basins – Beaufort Sea to Baja California,* Vol. 6, pp. 124–155, eds Scholl, D.W., Grantz, A. & Vedder, J.G., Circum-Pacific Council for Energy and Mineral Resources, Earth Science Series, Houston, Texas.

Scholl, D.W., von Huene, R. & Ryan, H.F., 2002. Basal subduction and the formation of the Aleutian Terrace and underlying forearc basin, in *Proceedings of the 3rd International Biennial Workshop on Subduction Processes*, UAF, June 10–14, 2002, Available at: http://www.whoi.edu/page.do?pid=20415&tid=282&cid=37947.

Scholl, D.W., Ryan, H.F. & von Huene, R., 2006. Exploring the notion that crustal thinning caused by subduction erosion formed the prominent deep-water forearc basin of the Aleutian Terrace, *Geol. Soc. Amer. Abstr. Prog.,* **38,** 4.

Seeber, L., Mueller, C., Fujiwara, T., Arai, K., Soh, W., Djajadihardja, Y.S. & Cormier, M.H., 2007. Accretion, mass wasting, and partitioned strain over the Dec 2004 Mw9.2 rupture offshore Aceh, northern Sumatra, *Earth planet. Sci. Lett.,* **263,** 16–31.

Sibuet, J.C., 2005. Les rapports de campagnes a la mer: MD149/Sumatra Aftershocks, pp. 105, Institut Polaire Francais, Available at: http://www.ifremer.fr/drogm_uk/Realisation/carto/Indien/Sumatra/Rap%20def%20sumatra1.pdf.

Sibuet, J.C., *et al*. 2007. 26th December 2004 great Sumatra-Andaman earthquake: co-seismic and post-seismic motions in northern Sumatra, *Earth planet. Sci. Lett.,* **263,** 88–103.

Sieh, K. & Natawidjaja, D., 2000. Neotectonics of the Sumatran fault, Indonesia, *J. geophys. Res.,* **105,** 28 295–28 326.

Singh, S.C., *et al*. 2008. Seismic evidence for broken oceanic crust in the 2004 Sumatra earthquake epicentral region, *Nat. Geosci.,* **1,** 777–781.

Smith, W.H.F. & Sandwell, D.T., 1997. Global sea floor topography from satellite altimetry and ship depth soundings, *Science,* **277,** 1956–1962.

Socquet, A., Vigny, C., Chamot-Rooke, N., Simons, W., Rangin, C. & Ambrosius, B., 2006. India and Sunda plates motion and deformation along their boundary in Myanmar determined by GPS, *J. geophys. Res.,* **111,** B05406, doi:10.1029/2005JB003877.

Song, T.A. & Simons, M., 2003. Large trench-parallel gravity variations predict seismogenic behavior in subduction zones, *Science,* **301,** 630–633.

Vigny, C., Socquet, A., Rangin, C., Chamot-Rooke, N., Pubellier, M., Bouin, M.-N., Bertrand, G. & Becker, M., 2003. Present-day deformation around Sagaing fault, Myanmar, *J. geophys. Res.,* **108,** 2533, doi:10.1029/2002B001999.

von Huene, R., Ranero, C.R. & Vannucchi, P., 2004. Generic model of subduction erosion, *Geology,* **32,** 913–916.

Washington, H.S., 1924. The lavas of Barren and Narcondam Islands, *Am. J. Sci., 5th ser, v.* **7,** 441–456.

Wells, R.E., Blakely, R.J., Sugiyama, Y., Scholl, D.W. & Dinterman, P.A., 2003. Basin-centered asperities in great subduction earthquakes: a link between slip, subsidence and subduction erosion? *J. geophys. Res.,* 2003, 2507. doi:1029/2002JB002072.

Wessel, P. & Smith, W.H.F., 1998. New improved version of Generic Mapping Tools released, *EOS, Trans. Am. geophys. Un.,* **79,** 579.